T.R.
VAN YÜZÜNCÜ YIL UNIVERSITY
INSTITUTE OF NATURAL AND APPLIED SCIENCES
DEPARTMENT OF CHEMISTRY

CONSTRUCTION OF PdRu NANOPARTICLES DECORATED REDUCED GRAPHENE OXIDE COMPOSITE FOR ELECTROCHEMICAL SENSING OF ENROFLOXACIN

M.Sc. THESIS

Aram Hamza IBRAHIM
Supervisor: Assoc. Prof. Dr. Adem ZENGİN

VAN – 2024

T.R.
VAN YÜZÜNCÜ YIL UNIVERSITY
INSTITUTE OF NATURAL AND APPLIED SCIENCES
DEPARTMENT OF CHEMISTRY

CONSTRUCTION OF PdRu NANOPARTICLES DECORATED REDUCED GRAPHENE OXIDE COMPOSITE FOR ELECTROCHEMICAL SENSING OF ENROFLOXACIN

M.Sc. THESIS

Aram Hamza IBRAHIM

Jury Members of the Thesis Defence Exam

Prof. Dr. Eylem TURAN (Chair)

Assoc. Prof. Dr. Adem ZENGİN (Supervisor)

Assoc. Prof. Dr. Muhammet GÜLER (Member)

VAN – 2024

ACCEPTANCE AND APPROVAL PAGE

This thesis entitled “Construction of PdRu Nanoparticles Decorated Reduced Graphene Oxide Composite for Electrochemical Sensing of Enrofloxacin” presented by Aram Hamza IBRAHIM under the supervision of Assoc. Prof. Dr. Adem ZENGİN in the department of chemistry, section analytical chemistry has been accepted as an M.Sc. thesis according to Legislations of Graduate Higher Education on 28/11/2024 with unanimity/majority of votes members of the jury.

Chair: Prof. Dr. Eylem TURAN Signature:

Member: Assoc. Prof. Dr. Adem ZENGİN Signature:

Member: Assoc. Prof. Dr. Muhammet GÜLER Signature:

This thesis has been approved by the committee of The Institute of Natural and Applied Sciences on ..……../...../…..….... with decision number of .....

Signature

…….

Director of Institute

ETHICAL DECLARATION

I declare that all the information in this thesis has been obtained and presented within the framework of ethical behavior and academic rules, and that in this thesis, which has been prepared in accordance with the thesis writing rules, all kinds of statements and information that do not belong to me have been fully cited.

Signature

Aram Hamza IBRAHIM

ABSTRACT

CONSTRUCTION OF PdRu NANOPARTICLES DECORATED REDUCED GRAPHENE OXIDE COMPOSITE FOR ELECTROCHEMICAL SENSING OF ENROFLOXACIN

IBRAHIM, Aram Hamza
M.Sc. Thesis, Department of Chemistry
Supervisor: Assoc. Prof. Dr. Adem Zengin
November 2024, 71 pages

In this study, a new electrochemical sensor depending on bimetallic nanoparticles palladium (Pd) and ruthenium (Ru) coated on the surface reduced graphene oxide glass carbon electrode (Pd@Ru/rGO/GCE), examined by surface analysis morphology SEM and EDX was constructed.

The results displayed that the obtained Pd@Ru/rGO nanoparticles have a uniform, compact morphology and were homogeneously distributed on the surface of rGO. The x-ray diffraction (XRD) and photoelectron spectroscopic (XPS) analyses were used to detect Pd and Ru. The data showed that the depositions of bimetallic nanoparticles on the surface rGO were successful. Pd@Ru/rGO/GCE was used for the detection of enrofloxacin; electrochemical sensitivity was 0.0291 μA μM^{-1}, and the linear range was estimated to be between 0.6 and 116 μM with a detection limit of 0.2 μM to detect enrofloxacin, indicating excellent performance and a low detection limit.

Experimental results show that prepared Pd@Ru/rGO/GCE exhibited excellent reproducibility and repeatability electrode, as well as high-stability Pd@Ru/rGO/GCE.

Keywords: Electrode fabrications, Electrochemical sensor, Electrochemistry, Enrofloxacin, Palladium (Pd)nanoparticle, Reduced graphene oxide, Ruthenium (Ru) nanoparticle, Sensor, Voltammetry

ÖZET

ENROFLOKSASİNİN ELEKTROKİMYASAL ALGILANMASI İÇİN İNDİRGENMİŞ GRAFEN OKSİT KOMPOZİTİNİ DEKOR EDEN PdRu NANOPARTİKÜLLERİNİN YAPISI

IBRAHIM, Aram Hamza
Yüksek Lisans Tezi, Kimya Anabilim Dalı
Danışman: Doç. Dr. Adem ZENGİN
Kasım 2024, 71 sayfa

Bu çalışmada, yüzeyi indirgenmiş grafen oksit cam karbon elektrot (Pd@Ru/rGO/GCE) üzerine kaplanmış paladyum (Pd) ve rutenyum (Ru) bimetalik nanopartiküllere bağlı yeni bir elektrokimyasal sensör, yüzey analizi morfolojisi SEM ve EDX ile incelendi.

Sonuçlar, elde edilen Pd@Ru/rGO nanopartiküllerinin düzgün, kompakt bir morfolojiye sahip olduğunu ve rGO yüzeyinde homojen olarak dağıldığını gösterdi. Pd ve Ru'yu tespit etmek için X-ışını kırınımı (XRD) ve fotoelektron spektroskopik (XPS) analizleri kullanıldı. Veriler, bimetalik nanopartiküllerin rGO yüzeyindeki birikimlerinin başarılı olduğunu gösterdi. Pd@Ru/rGO/GCE, enrofloksasinin tespiti için kullanıldı; elektrokimyasal duyarlılık 0.0291 μA μM^{-1} idi ve doğrusal aralığın 0.6 ile 116 μM arasında olduğu ve enrofloksasini tespit etmek için 0.2 μM'lik bir tespit limiti ile mükemmel performans ve düşük bir tespit limiti gösterdiği tahmin edildi.

Deneysel sonuçlar hazırlanan Pd@Ru/rGO/GCE'nin mükemmel tekrarlanabilirlik ve tekrarlanabilirlik elektrodu ve yüksek kararlılığa sahip Pd@Ru/rGO/GCE sergilediğini göstermektedir.

Anahtar kelimeler: Elektrokimya, Elektrokimyasal sensör, Elektrot imalatı, Enrofloksasin İndirgenmiş grafen oksit, Paladyum (Pd) nanopartikül, Rutenyum (Ru) nano - partikül,Sensör, Voltammetric

ACKNOWLEDGMENT

I would like to thank This MSc thesis would have been impossible to perform without a group of people who supported me, helped me, and advised me throughout its development. I wish to demonstrate my profound regard and respect to the Assoc. Prof. Dr Adem Zengin, my MSc thesis supervisor.

I wish to share my significant regard and respect for the Assoc. Prof. Dr. Muhammet Guler, for her kind guidance, enthusiastic backing, and insightful criticism of this study.

I would also like to thank the Head of the Institute of natural and applied sciences for their guidance and assistance to ensure my progress remains aligned.

Finally, my thanks are also extended to the chemistry department's staff and instructors for enabling me to visit them anytime to get information. My parents' steadfast confidence in my capabilities as a student has been helpful, and I am profoundly appreciative of their support.

2024

Aram Hamza IBRAHIM

CONTENTS

Page

ABSTRACT i
ÖZET iii
ACKNOWLEDGMENT v
CONTENTS vii
LIST OF TABLES ix
LIST OF FIGURES xi
SYMBOLS AND ABBREVIATIONS xiii
1. INTRODUCTION 1
1.1 Enrofloxacin 5
1.2 Voltammetry; Cyclic Voltammetry and Differential Pulse Voltammetry 7
1.3 Palladium and Ruthenium 8
1.4 Electrochemistry Related to The Nanoparticles 9
2. LITERATURE REVIEW 11
3. MATERIALS AND METHODS 15
3.1 Materials 15
3.2 Methods 15
3.2.1 Synthesis Pd/rGO 15
3.2.2 Synthesis Ru/rGO 16
3.2.3 Synthesis Pd@Ru/rGO 16
3.2.4 Synthesis Electrode fabrication Sensor 17
4. RESULTS 19
4.1 SEM and EDX Results 19
4.2 XRD Results 20
4.3 XPS Results 22
4.4 Electrochemistry Results 24
5. DISCUSSION AND CONCLUSION 33
REFERENCES 37
EXTENDED TURKISH SUMMARY 43
CURRICULUM VITAE 47

LIST OF TABLES

Page

Table 1.1 Enrofloxacin's physicochemical properties (Grabowski et al., 2022) 6
Table 4.1 According to pattern Figure 4.4, each element has the top percentage ratio of atomics..... 22
Table 4.2 Detection of ENR in ENR containing tables..... 31
Table 5.1 This table compares this study and reviews each paper due to the linear range, LOD, and peak potential reported in this table..... 35

LIST OF FIGURES

Page

Figure 1.1 GO preparation and usage scheme (Kumar et al., 2021) 2
Figure 1.2 Graphene oxide Lerf-Klinowski model (Lerf et al., 1998) 3
Figure 1.3 Diagram showing the mechanism structure change of graphene to produce GO and rGO (Ławkowska et al., 2021; Liu et al., 2022) 5
Figure 1.4 Depicts the mechanism of action of enrofloxacin (Kohanski et al., 2010) 6
Figure 4.1 SEM image of Pd@Ru/ rGO from low magnification into high magnifications..... 19
Figure 4.2 EDX mapping image 1 um of Pd@Ru/rGO 20
Figure 4.3 XRD patterns: The red one is Pd@Ru/rGO, and the black one is rGO 21
Figure 4.4 Broad survey range scan spectrum of XPS Pd@Ru/ rGO 23
Figure 4.5 Cyclic voltammograms of (a) GCE, (b) rGO/GCE, (c) Pd/rGO/GCE, (d) Ru/rGO/GCE, and Ru/Pd/rGO/GCE obtained in 5 mM $[Fe(CN)_6]^{3-}$/ $[Fe(CN)_6]^{4-}$ containing 0.1 M KCl at 0.05 V/s 24
Figure 4.6 (a) Cyclic voltammograms of (a) GCE, (b) rGO/GCE, (c) Pd/rGO/GCE, (d) Ru/rGO/GCE, and Ru/Pd/rGO/GCE obtained in BR buffer (pH 5.0) in the absence (a) and presence of 0.1 mM ENR (b)..... 25
Figure 4.7 (a) Linear sweep voltammograms of Ru/Pd/rGO/GCE obtained in BR buffer with various pH values (3.5-7.0) in the presence of ENR (b) current versus pH graph and potential versus pH graph..... 26
Figure 4.8 (a) Cyclic voltammograms obtained on Ru/Pd/rGO/GCE in BR buffer (pH 5.0) containing ENR at various scan rates (from 0.04 to 0.30 V/s) (b) current versus scan rate graph..... 27
Figure 4.9 (a) Differential pulse voltammetric response of Ru/Pd/rGO/GCE in BR buffer (pH 5.0) to ENR (b) current versus concentration of ENR graph (deposition potential: 0.5V, deposition time: 90 s, scan rate: 0.01 V/s, modulation amplitude: 0.025 V, modulation time: 0.05 s)..... 28
Figure 4.10 (a) Repeatability and (b) reproducibility results of Ru/Pd/rGO/GCE..... 29

Figure 4.11 (a) Differential pulse voltammetric results of ENR were obtained on Ru/Pd/rGO/GCE electrochemical sensor (b) current versus the concentrations used in the ENR graph..... 30

SYMBOLS AND ABBREVIATIONS

Some symbols and abbreviations used in this thesis are presented below, along with their descriptions.

Symbols	Description
α	Alpha (Mmol/G.Min)
µ	Micro
µA	Microampere
µL	Micro litter
µM	Micrometer
A	Cm^2 Current
ev	Electron volt
I_p	Ampere
Kd	Dispersion Coefficient
mg	milligram
Min	Minute
Ml	Milliliter
mM	Millimole
Nm	Nanometer
P	Potential
R%	Removal Efficiency
R^2	The Coefficient of Determination
RSD	relative standard deviation
S/N	Sanalytesnoise
SD	standard deviation
T	Temperature (Celsius)

Abbreviations	Description
AuNPs	Gold nanoparticles
$CaWO_4$/RGO (CW/RGO)	Calcium tungsten oxide/reduced graphene
CoCH-6 h/GCE	Cobalt-based hybrid-modified glassy carbon electrode
COF	Covalent organic framework
CV	Cyclic voltammetry
DPV	Differential pulse voltammetry
EDX	Energy dispersive analysis
ENR	Enrofloxacin
GCE	Glass carbon electrode
LOD	Limit of Detection
MIP	Molecular Imprinting Polymers
MIT	Molecular Imprinting Technology
MWCNTs/MIPS/	Multiwalled carbon nanotubes/Molecularly imprinted polymers
NIP	Non-Imprinting Polymers
Pd	Palladium
PDA	P-phthalaldehyde
rCNT/GCE	Reduced carbon nanotubes/glass carbon electrode
rGO	Reduce graphene oxide
Ru	Ruthenium
SEM	Scanning Electron Microscope
TAPB	3,5-tris(4-aminophenyl)benzene
XPS	X-ray fluorescence analysis
XRD	X-ray diffraction analysis

1. INTRODUCTION

Graphene is one of the most researched materials, and it is called the material of the future due to its unique properties. All of the constituents of graphene are carbon atoms, joined in a honeycomb network by sp2 hybridized orbitals that link each carbon atom to three distinct carbon atoms for a variety of uses, such as field-effect transistors, gas, and biomolecule sensors, transparent conductive films, and graphene batteries. Graphene is an auspicious material because of its rarity (Rümmeli et al., 2011).

Graphene oxide (GO) is a layered carbon structure with oxygen-containing functional groups (=O, -OH, -O—, -COOH) that adhere to the plane's edges and sides. GO can have a monolayer or multilayer structure like any two-dimensional carbon material. One layer of graphene oxide consists of one layer, and double-layer graphene oxide (double-layer GO) consists of two layers. Multilayer graphene oxide has two or more layers (Wang et al., 2011).

Graphite oxide is produced by oxidizing graphite and subsequently exfoliating the resultant graphite oxide to obtain graphite oxide. The synthesis process significantly influences the material properties by altering the quantity and type of oxygen-containing groups generated in graphene oxide. Since graphene is not hydrophilic like GO is, it is easier to prepare suspensions based on organic or water-based solvents, with a band gap of roughly 2.2 ev, highly oxidized GO functions as an electrical insulator. Because graphene oxide has multiple oxygen functionalities on its surface, it can be used as a precursor to create a wide range of graphene derivatives, including fluorographene, Bromo graphene, and graphene. GO can also be reduced chemically or thermally to produce thermally or chemically reduced graphene oxide. (Figure 1.1) GO can also be utilized in cutting-edge applications like construction materials, high-temperature materials, and medication delivery. Certain issues still require improvement and closer examination. It is critical to create new techniques for the large-scale, inexpensive, environmentally friendly synthesis of GO. The importance of graphene oxide is due to; GO structure, GO synthesis and characterization, and GO functionality. (Figure 1.1) (Kumar et al., 2021).

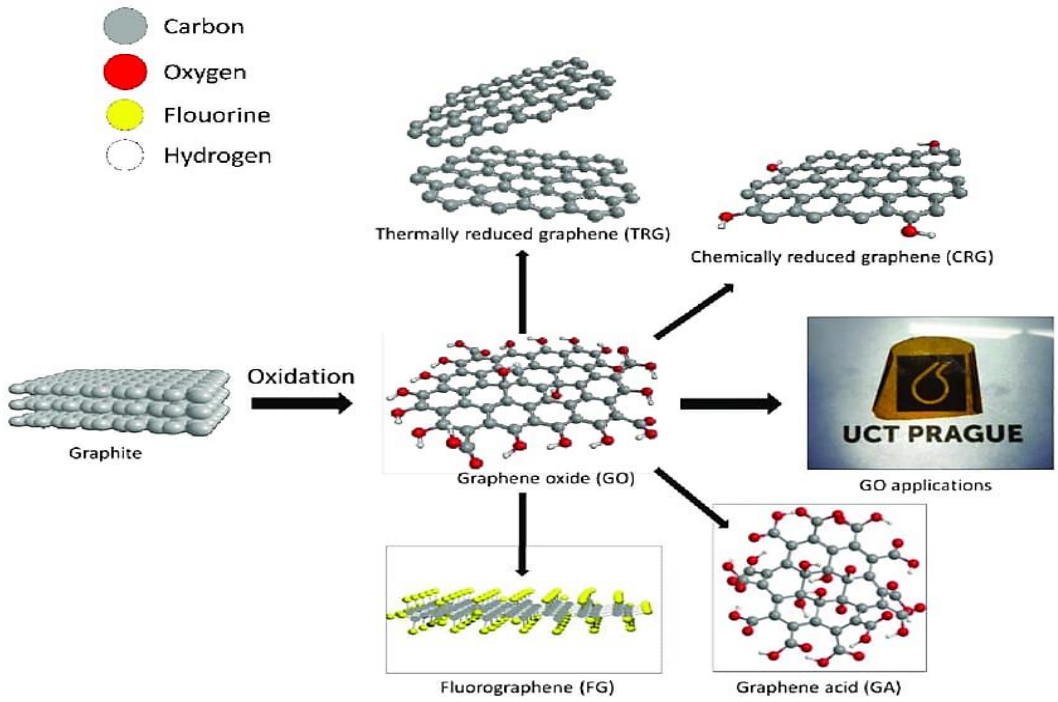

Figure 1.1 GO preparation and usage scheme (Kumar et al., 2021)

LK is a model that in 1998, Leroff and Klinovsky created, which consists of two different kinds of regions (Figure 1.2); The degree of oxidation of the substance determines the size of the two regions, areas containing unoxidized benzene aromatic rings and areas with six-membered aliphatic rings. The model is dominated by double bonds, epoxide groups, and aromatics. The distortions in the monolayer result from the slightly altered tetrahedral arrangement of the hydroxyl groups bonded to the carbon atoms; two layers of oxygen atoms with varying concentrations are produced when Functional oxygen groups are affixed to the carbon monolayer on both the upper and lower surfaces, these layers are primarily made up of hydroxyl and epoxide groups, which are extremely close to one another. All oxygen functionalities, aromatics, and oxidized rings are dispersed erratically throughout the carbon monolayer. The acidity of GO is attributed to the hydroxyl and carboxyl groups attached to the lattice edges; many people use and accept this LK model for somewhat oxidized GO (Lerf et al., 1998).

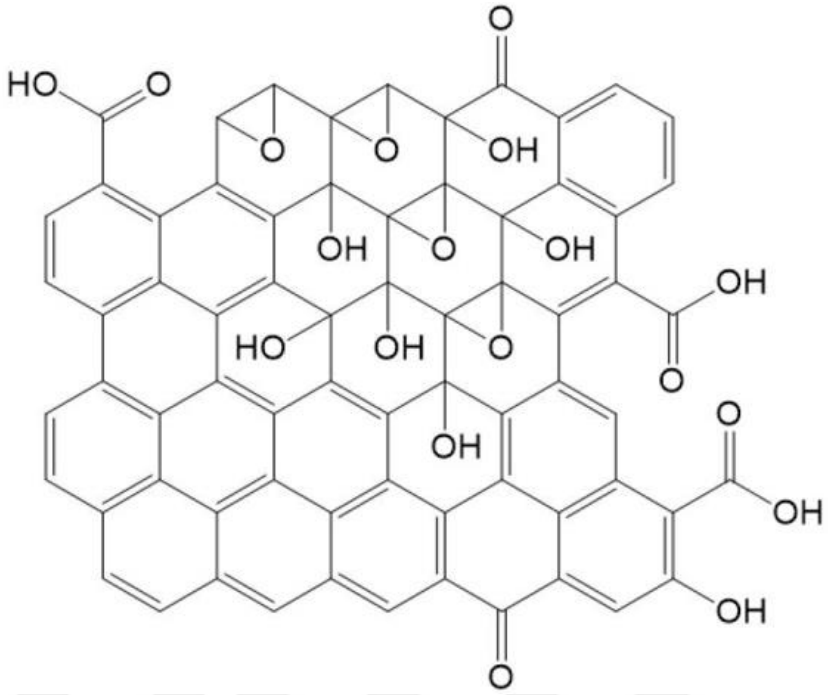

Figure 1.2 Graphene oxide Lerf-Klinowski model (Lerf et al., 1998)

Reduced graphene oxide is produced by chemically or thermally reduced graphene oxide by the Hummer method, which is practically prepared by 27 ml of sulfuric acid (H_2SO_4) and 3 ml of phosphoric acid (H_3PO_4) the volume ratio 9:1 mixed and needed to stir for several minutes. Then 0.225 g of graphite powder was added into the mixing solution under stirring conditions. 1.32 g of potassium permanganate ($KMnO_4$) was then added slowly into the solution. Although rGO has improved electrical conductivity compared to GO, it does not reach the same level as pristine graphene. Its partially restored structure allows it to maintain a balance between conductivity and processability. Applications include supercapacitors, batteries, sensors, and conductive coatings. Graphite is oxidized to produce graphene oxide, and then the graphene oxide is reduced to produce reduced graphene oxide (Smith et al., 2019).

Graphene oxide applications:

Air pollution constitutes one of the most significant threats to the environment, which is brought on by the emission of dangerous industrial gases like CO_2, CO, NO_2, and NH_3. Because the base's edges and surfaces are decorated with oxygen groups, GO can interact both covalently and non-covalently with a variety of molecules. GO can be utilized as a catalyst in industrial processes to change harmful gases, such as hazardous

gases, that can be eliminated by directly using gas conversion catalyst reactions or gas absorption and storage. After gas pollution, water contamination ranks high among the most pressing environmental issues (F. Li et al., 2015).

The potential use of GO in the medical and biological fields is through GO-based biosensors. Instead of double-stranded DNA, single-stranded DNA interacts with GO-based biosensors for their detection. The effective helical structure of dsDNA conceals core bases, preventing GO from interacting directly with core bases (Lu et al., 2009; S. He et al., 2010; Cui et al., 2012).

GO Membranes: GO membranes can selectively transport gases while also serving as ionic and molecular sieves. Materials at high temperatures GO: Materials that strengthen and enhance the Mechanical characteristics of high-temperature materials include graphene and graphene oxide. GO 1% by volume can yield a notable increase in mechanical strength. Graphene oxide powder was dispersed within an AlMg5 hub alloy matrix utilizing a high-energy mill. A hot press was used to compact the materials that were obtained (Kwon et al., 2017).

GO and construction materials: Ordinary Portland cement is among the most prevalent materials utilized in civil engineering. Due to its tendency towards urbanization. Aggregates, an adhesive (OPC), and water of hydration are the ingredients that go into making concrete. Concrete has certain benefits, like its exceptional compressive strength, but it also has drawbacks, like low tensile strength or poor crack resistance (Chuah et al., 2014).

GO can be reduced thermally, chemically, or electrochemically. Compared to GO, rGO has a higher electrical and thermal conductivity because fewer equipment groups are present. Generally, in theory, rGO can form one-atom-thick graphene by decreasing the group. Still, rGO has certain shortcomings in comparison to pure graphene. As an illustration, rGO exhibits stone - wells defects, or a pentagonal/hexagonal bonded carbon atom lattice, which significantly affects the physicochemical properties. Interestingly, because of the increased density of states brought about by defects in the graphene basal plane, these defects—which were previously thought to be the source of the reduced conductivity—may help with electron transport (Figure 1.3). As a result, striking a balance between the rise in density of states and the decrease in conductivity reduced

graphene oxide with a moderate defect density exhibits a rapid electron transfer rate (Ławkowska et al., 2021; Liu et al., 2022).

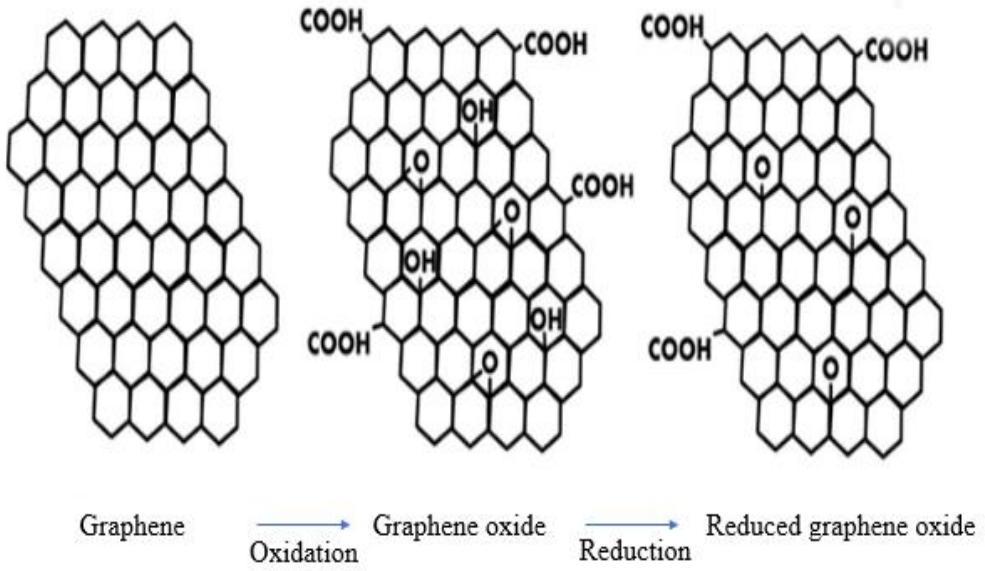

Figure 1.3 Diagram showing the mechanism structure change of graphene to produce GO and rGO (Ławkowska et al., 2021; Liu et al., 2022)

1.1 Enrofloxacin

ENR is a fluoroquinolone antibiotic widely used in veterinary medicine. Enrofloxacin is a very lipophilic compound and the addition of a carboxylic acid and a tertiary amine increases its amphoteric properties (Kohanski et al., 2010).

Strong antibacterial efficacy against gram-positive and gram-negative microorganisms is primarily because bacterial gyrase and topoisomerase IV inhibit enzyme activities. The high efficiency of this molecular structure has been shown in the treatment of all kinds of animals in farms and other environments.

On the other hand, ENR has serious side effects including skeletal, reproductive, immune, and digestive problems. Enrofloxacin is a 1,4-dihydroquinoline-3-carboxylic acid also known as quinoline monocarboxylic acid. In addition, this antibiotic consists of a quinoline monocarboxylic acid (Grabowski et al., 2022). Table 1.1 displays its critical physical and chemical characteristics.

Table 1.1 Enrofloxacin's physicochemical properties (Grabowski et al., 2022)

Property	**Value**
Molecular formula	$C_{19}H_{22}FN_3O_3$
Molecular weight	359.3 g/mol
Chemical safety	Health risks, environmental risks, and irritants
Color/form	Pale yellow crystals
Melting point	220 °C

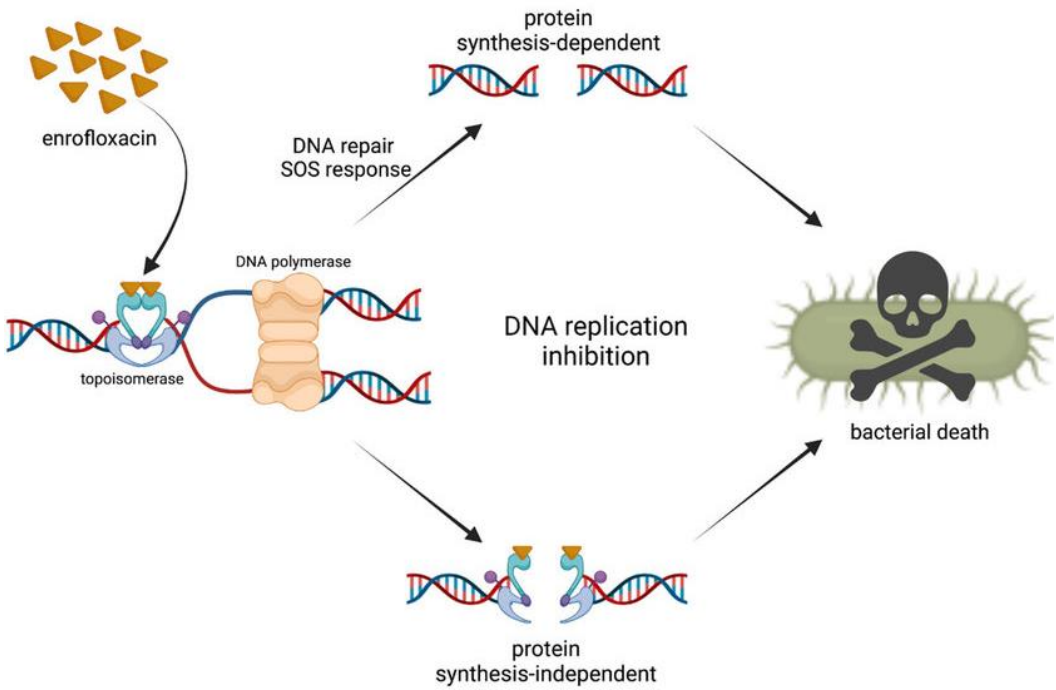

Figure 1.4 Depicts the mechanism of action of enrofloxacin (Kohanski et al., 2010)

Enrofloxacin's mechanism of action attaches to the DNA-topoisomerase complex at the cleavage locus. This causes conformational abnormalities in the enzyme cutting and binding that lead to inefficient DNA. Depending on the concentration, cell death, DNA repair mechanisms, and S.O.S. Answers are activated. Reproduced with modifications by ref (Kohanski et al., 2010).

Enrofloxacin exhibits a biphasic concentration-response curve;

• In the first stage, increasing the concentration of enrofloxacin leads to a greater proportion of bacteria being killed.
• As the concentration of enrofloxacin is raised in the second phase, the rate of bacterial death decreases.

1.2 Voltammetry; Cyclic Voltammetry and Differential Pulse Voltammetry

The study of current as a function of applied potential is known as voltammetry. Cyclic voltammetry is a popular technique for identifying the procedures involving oxidation and reduction of a specific molecular species as well as providing information on electron transfer - initiated chemical reactions (Elgrishi et al., 2018).

CV process is putting a potential on a substance and then measuring the current that flows through it. This fact allows the calculation of several electrochemical variables, including reaction rate, diffusion coefficient, and reactive potential kinetics, as well as information about the reversibility of redox reactions. Voltametric methods for electrochemical cells are used to study reactions that occur at the electrode/electrolyte interface. The reactivity of the analyte in these half-cells is used for quantification. The applied potential changes over time and the corresponding changes in current are measured, making it a dynamic electrochemical method voltammetry consists of three electrode sources; a working electrode, a reference electrode, and an auxiliary electrode (Abd El-Hady et al., 2019; El Gindy et al., 2022).

A voltammogram is a graph that shows the current of an electrochemical cell as a function of the applied potential. Concentration is determined by reading graph values, like limiting or peak current, and plugging them into different mathematical models. The standard potential can be calculated using the Nernst equation. Applied after determining the concentration. There are three main types of voltammograms. Before shaping, the diffusion layer was determined. If the analyte is continuously stirred, the emission will have a constant width, producing a constant current voltammogram. As the current increases from the residual background to the limiting current. If the mixture is not stirred, the width of the diffusion layer increases with time. This is represented by the maximum peak current, which is represented by the highest point on the graph. A third common form of voltammogram measures the sample for changing current rather than applied

current. In general, cyclic voltammetry is an effective technique for studying the complex interactions of metal ions and organic ligands (Al-Harazie et al., 2024).

Differential pulse voltammetry (DPV) is a technique that involves applying amplitude potential pulses to a linear ramp potential. In DPV, a voltage that does not undergo a faradaic reaction is selected and then applied to the electrode. The base potential is raised in equal amounts between pulses. The current is measured immediately before and after the pulse application, and then the difference is recorded (Baldwin et al., 1986) .

1.3 Palladium and Ruthenium

Palladium is a rare and shiny silvery-white metal and chemical element with the symbol Pd and atomic number 46. Palladium compound oxidation states exist primarily in the 0 and +2. Pd has the lowest density and melting temperature among these elements. Pd is currently most frequently used in automobile catalytic converters. In catalytic converters, noble metals are utilized to transform automobile emissions of nitrogen oxide, hydrocarbons, and carbon monoxide into nitrogen and carbon dioxide (Zereini and Alt, 2006).

Pd-based alloy clusters and nanoparticles have garnered interest. Pd nanoparticles are a flexible catalyst that can be used in a variety of organic reactions, including hydrogenation (Favier et al., 2020). Palladium can also be used in hacking and Suzuki coupling, creating bonds between carbon atoms (Heck and Nolley, 1972; Suzuki et al., 1979). A major discovery in organic synthesis; Pd-catalyzed in across-coupling reactions, were other uses for Pd nanoparticles including fuel cells, hydrogen sensing and storage, and the catalysis of organic reactions (Antolini, 2009; Adams and Chen, 2011). Another possible palladium electronic application is sensors that can be coated on the surface of graphene oxide (Silva et al., 2012). Due to the use of palladium as an NP in the reactions, many biomedical applications have also been developed or discussed, including photothermal, antibacterial, and anticancer therapies (Phan et al., 2019).

Ruthenium belongs to the platinum group indicated in the periodic table of transition metals, with the atomic number 44. It has appeared silvery-white appearance, high hardness, and excellent corrosion resistance. Found in ores along with other

platinum-group metals, ruthenium exhibits unique catalytic, electrical, and chemical properties, making it valuable for diverse industrial and scientific applications. Physical and Chemical Properties, symbol: Ru, atomic number: 44, melting point: (2.334 °C), density: 12.45 g/cm³, oxidation states: 0, +2, +3, and +4. Chemical stability: highly resistant to oxidation and corrosion, especially at room temperature.

Applications of ruthenium include catalysis, hydrogen evolution reactions, oxygen evolution reactions, ammonia synthesis, ethanol and CO oxidation electronics, hard disk drives, electrical contacts, chemotherapy, ruthenium-based complexes supercapacitors, and RuO_2 (ruthenium oxide) batteries, jewelry, and Coatings (Clarke, 2003).

1.4 Electrochemistry Related to The Nanoparticles

Metal nanoparticles are used for catalysis, energy conversion, storage, and sensors. The size, shape, and surface adhesion of nanoparticles significantly impact their electrocatalytic activity. Efforts to investigate electrochemistry in individual nanoparticles have included immobilizing a nanoparticle on a small electrode's surface, transporting single nanoparticles to electrode surfaces, and measuring the catalytically enhanced current generated by random particle collisions with the electrode surface. Despite the signals obtained in these experiments being produced by individual nanoparticles, acquiring spatially and temporally resolved information regarding heterogeneous processes within a specific nanoparticle is difficult due to characterization issues and the challenge of distinguishing a single particle from other nanoparticles in the system. It made things challenging. Nano electrochemical instruments with distinctive dimensions smaller than or equivalent to the target particle are required to conduct electrochemical experiments on a single NP and characterize it in situ (Mirkin et al., 2016).

In the twenty-first century, nanotechnology has developed as a scientific advancement. This field encompasses the synthesis, administration, and application of materials measuring less than 100 nm. Wastewater treatment is one of the many industries where nanoparticles find extensive use, including the environment, agriculture, food, biotechnology, biomedicine, and medicine (Zahra et al., 2020). A material particle with a diameter ranging from one to one hundred nanometers is termed a nanoparticle.

Nanoparticles often exhibit unique size-dependent characteristics due to their diminutive dimensions and extensive surface area. When a crystalline particle's size gets closer to the nanoscale and its characteristic length scale is smaller than or equal to the de Broglie wavelength or the wavelength of light, the particle's periodic boundary condition is lost (Luo and Wang, 2014).

Since pH is essential to many chemical processes, it is widely required in labs, clinics, and industry. As a result, in many applications, quick, precise, and trustworthy pH measurement is crucial. Numerous methods exist for measuring pH, but the most popular ones that employ oxides as pH-sensitive layers are conductance/capacitance field-effect transistors, potentiometric, and ionic methods. The technique is more widely used because it is easier to make and has been around for a longer time (Zaman et al., 2011).

2. LITERATURE REVIEW

For example, many electrochemical sensors have been fabricated to detect enrofloxacin. The fabrication produces molecularly imprinted polymers with the modification of a screen-printed gold electrode estimated by square wave voltammetry, which measures the oxidation peak when at +0.9 V the linear range of enrofloxacin is 0.01-0.1 mM, and its LOD is 0.02 mM. The benefit of this modification is that sample running no longer requires analyzing and detecting molecules; it is simple and easy to detect enrofloxacin (Gallegos-Tabanico et al., 2022).

Another study for the detection of enrofloxacin is the fabrication of multiwalled carboxylate carbon nanocomposites of reduced graphene oxide with carbon nanotubes (MWCNT-COOH-RGO) electrochemical sensor, a sensitive electrochemical technique was created using a bare electrode of graphene oxide and enrofloxacin reduced with carboxylate carbon nanotubes. These electrodes were identified by molecular recognition imprinted with them and direct electrocatalytic oxidation, respectively. The detection limit is 2.3×10^{-7} M and the linear range is 5.0×10^{-7} M to 5.5×10^{-5} M (Wu et al., 2023).

Another example involves the detection of enrofloxacin using cyclic voltammetry and differential pulse voltammetry, along with a comprehensive investigation of the electrochemical sensor's performance. Enrofloxacin detection was found to be correlated with the number of printed polymers and the pH of the electrolyte. The sensor's differential pulse voltammetry response current had an excellent linear relationship at 0.2 V. The experimental connection was a three-electrode system with the modified electrode as the working electrode when the concentration of enrofloxacin was 2.8 pM–28 μM, and the detection limit was 0.9 pM (Chen et al., 2022a).

As an organic linker, 2,3,6,7,10,11-hexaaminotriphenylene (HATP) used to compare Co3(HITP)2 and Ni3(HITP), CoxNi3-x(HITP)2 has metallic compounds of $Co^{2+}/Co^{3+}/Ni^{2+}/Ni^{3+}$ synthesis and design it. A CoNi-based metal-organic semiconductor (MOF), CoxNi3-x(HITP)2, is very important in the construction of MOF-based sensors for food safety, medical diagnosis, and environmental protection, with a detection limit is 0.2 fg. mL^{-1} and linear range of 0.0011 pg•mL^{-1}. It has a high selectivity, good reproducibility, good stability, and a lot of different uses of an electrochemical aptasensor based on enrofloxacin exhibits superior sensing performance (Song et al., 2021).

The present study compares two electrochemical methods for the identification and measurement of enrofloxacin in the presence of possible interferents, including ciprofloxacin, and humic acids from ralun and frutillar. The findings demonstrate that, due to their high linearity, detection, and quantification capabilities, electrochemical techniques like square wave and cyclic voltammetry may be more helpful than conventional methods for the detection and quantification of this antibiotic in the soil-solution matrix when the above interferences are present. It creates the possibility of using these electrochemical devices as potential amperometric sensors because of the complementary use of other techniques (Canales et al., 2019).

Using cyclic voltammetry (CV) and a novel molecular polymer called poly(pyrrole-co-ve-phenylenediamine) (p(Py-co-OPD), an enrofloxacin (ENR) sensor was fabricated. When the detection limit is low (6.57×10^{-13} mol/L towards ENR) and the linear range between 1.0×10^{-4}-1×10^{-10} mol/L, the MIP sensor employs square wave voltammetry that the condition depends on pH level, the concentration of enrofloxacin, the number of CV cycles, extraction solution of the template and the incubation the sensor it was used to determine the ENR amount in the pharmaceutical samples with satisfactory result (Yan et al., 2017).

In this study, milk and river water samples contained enrofloxacin, with a linear range between 0.001-115 M and a minimum (LOD) of 0.021 M. The CaWO4/rGO nanocomposite (CW/rGO) was made using a basic tool; good selectivity, outstanding long-term stability, and excellent reproducibility are the goals of the hydrothermal method. The benefit of using the hydrothermal method for preparing the CW/rGO nanocomposite was its electrocatalytic performance The goals of the hydrothermal method are good selectivity, great long-term stability, and great reproducibility., which allowed for the electrochemical detection of the antibiotic drug enrofloxacin. Two methods were used to study the electrocatalytic oxidation performance of enrofloxacin: amperometry (AMP) measurement and cyclic voltammetry (Chen et al., 2022b).

A CoNi-based metal-organic framework (MOF) and gold nanoparticles (AuNPs) were used in this study to make an electrochemical apt sensor that can detect enrofloxacin (ENR) very quickly. Characterization techniques such as the scanning electron microscope, Fourier-transform infrared spectrophotometer (FT-IR), and x-ray diffraction (XRD) were used to optimize Co-MOF, Ni-MOF, and CoNi-MOF. Electrochemical

behavior was studied using cyclic voltammetry (CV) and the electrochemical impedance spectrum (EIS). The linear range of Apt/AuNPs/CoNi-MOF/GCE between 1×10^{-3} pg·mL^{-1} to 1×10^{-5} pg·mL^{-1} (S/N = 3) and a detection limit of 3.3×10^{-4} pg·mL^{-1} for ENR at optimal conditions. The configured sensor exhibits high sensitivity, excellent reproducibility, and prolonged stability. The acquired sensor demonstrates significant potential for the sensitive detection of ENR in meat samples (Wei et al., 2022).

An innovative electrochemical aptasensor utilizing a bimetallic organic framework-derived carbide nanostructure composed of cobalt and nickel ($NiCo_2O_4$@NiO). Electrochemical impedance Spectroscopy and cyclic voltammetry were employed to evaluate the affection of the electrochemical sensor. To detect Enrofloxacin with a low detection limit of 1.67×10^{-2} pg mL^{-1} and linear range between 5×10^{-2} to 5×10^{-4} pg mL1.The morphology and structure of the material were characterized using scanning electron microscopy and x-ray photoelectron spectroscopy, while solvothermal and direct pyrolysis methods were applied to a modified electrode to enhance the electron transfer efficiency of the fabricated electrode (Niu et al., 2023).

3. MATERIALS AND METHODS

3.1 Materials

Reduced graphene oxide (rGO), potassium tetrachloropalladate (II) K_2PdCl_4, ruthenium (III) chloride hydrate ($RuCl_3$) nH_2O, sodium borohydride ($NaBH_4$), enrofloxacin ($C_{19}H_{22}FN_3O_3$), absolute ethanol (CH_3CH_2OH), distilled water (D.W), buffer solution (BR), ($K_4[Fe(CN)_6]$), ($K_3[Fe(CN)_6]$), KCl, and also using these glassware and devices; magnetic stirrer, analytical precision balance (precise), vacuum oven (EV 018), SEM and EDX (scanning electron microscope) (Zeiss Evo 15 Model), XRD, XPS, CV, distilled water, filter paper, micropipette and drip tip and pipette filer, beaker, micropipette transfer, funnel, and conical flask, clamp and stand, spatula, fume hood, magnetic stirrer and magnetic bar, paraffin, collection tube, washing bottle, ice water, sonication device, pH meter device, glass carbon electrode tube (GCE).

3.2 Methods

3.2.1 Synthesis Pd/rGO

100 mg of rGO was added to a beaker that contained 20 ml distilled water, after addition to dispersion, sonicated for one hour, to dispersion all rGO in the water solution after sonication 16 mg of potassium tetrachloropalladate (II). K_2PdCl_4 and addition to a container that contains 5 micro-distilled water solution sonication to 5 minutes then the tube is added into the rGO solution and stirred for 1 hour. Dissolved 49 mg of $NaBH_4$ in 1ml distilled water, sodium hydroborate (reducing agent to produce Pd ion) slowly drop by drop and add to the mixture that contains K_2PdCl_4, and rGO then sonication 3.5 hours after that filtered by filter paper and a washing process done several times approximately 150 ml D.W and at finally by absolute ethanol (100 ml ethanol) to remove any impurities. After drying the precipitate was used to compare after synthesis Pd/ rGO GCE with Ru/ rGO/ GCE and Pd@Ru/ rGO GCE to detect enrofloxacin.

3.2.2 Synthesis Ru/rGO

100 mg of rGO was added to a beaker that contained 20 ml distilled water, after addition to dispersion, sonicated for one hour, to dispersion all rGO in the water solution, after sonication 10.2 mg of ruthenium (III) chloride hydrate. $RuCl_3$. nH_2O was added to a container containing 5 micro-distilled water solution sonication for 5 minutes. Then, the tube was directly added to the rGO solution and stirred for 1 hour. Dissolved 49 mg of $NaBH_4$ in 1ml distilled water, sodium hydroborate (reducing agent to produce Ru ion) slowly drop by drop and add to the mixture that contains ruthenium (III) chloride hydrate. $RuCl_3$. nH_2O, and rGO then sonication 3.5 hours after that filtered by filter paper and a washing process done several times, approximately 150 ml D.W, at the final step by absolute ethanol (100 ml ethanol) to remove any impurities. After drying the precipitate was used to compare after synthesis Ru/ rGO with Pd/ rGO GCE GCE and Pd@Ru/ rGO GCE to detect enrofloxacin.

3.2.3 Synthesis Pd@Ru/rGO

100 mg of rGO was added to a beaker that contained 20 ml distilled water and dissolved, after addition to dispersion, it was sonicated for one hour, to dispersion all rGO in the water solution. After sonicated 16mg of potassium tetrachloropalladate (II). K_2PdCl_4, and addition to a container that contains 5 micro-distilled water solution sonication to 5 minutes, moreover it is similar for 10.2 mg ruthenium (III) chloride hydrate ($RuCl_3$. nH_2O) is added to a container that contains 5 micro-distilled water solution sonication for 5 minutes, and then each tube is incorporated into the rGO solution and agitated for one hour. Dissolved 98 mg of $NaBH_4$ in 1ml distilled water, sodium hydroborate (reducing agent to produce pd ion and Ru ion) slowly drop by drop and add to the mixture that contains K_2PdCl_4, $RuCl_3$. nH_2O and rGO then sonication 3.5 hours after that filtered by filter paper and a washing process done several times, approximately 150 ml D.W and finally absolute ethanol (100 ml ethanol) to remove any impurities then collected all samples were then put into a vacuum oven for 24 hours characterized by SEM, XPS, and XRD, and used electrochemistry to synthesize Pd@Ru/rGO GCE and application electrochemistry to detect enrofloxacin and real sample baytril tablet.

3.2.4 Synthesis Electrode fabrication Sensor

Preparation buffer solution: 2.0, 2.5, 3.0, 3.5, 4.0, 4.5, 5.0, 5.5, 6.0, 6.5, 7.0, 7.5, 8.0, 8.5 to detection working area at PH:5.0 then preparation of the following solution to compare electrode 0.2112 g of $K_4[Fe(CN)_6]$, 0.1646 g of $K_3[Fe(CN)_6]$, and 0.7456 g KCl. All of it is prepared in the 100 ml D.W to compare of pH electrode, Finally, after optimization pH range, PH is:5.0.

After prepared 5 electrodes; Bare electrode, rGO/GCE, Ru/ rGO/GCE, Pd/ rGO /GCE, Pd@Ru/ rGO /GCE each electrode is prepared by the following steps the applied to the voltammetric device; rGO/GCE electrode is prepared with 20 mg of rGO, then added to 5 ml D.W, and sonicated for 30 minutes to disperse, shaking the mixture well for 1 minute. After that take 10 micros into the working electrode, Put the working electrode into a vacuum oven, and -0.2 until 10 minutes then it is ready to work. It is similar to preparing all electrodes: Bare electrode Ru/ rGO/GCE, Pd/ rGO /GCE, Pd@Ru/ rGO /GCE.Used a real sample and received stable and accurate data with a low detection limit.

4. RESULTS

4.1 SEM and EDX Results

SEM and EDX are the most recognized and extensively utilized techniques for surface analysis. Some advantages of SEM and EDX are that micro-areas are among the most important test instruments for in-situ analysis, strong stereoscopic vision, high magnification, a wide depth of field, high resolution, and precisely concentrated scanning electron beam is employed to produce high-resolution images of surface topography with exceptional depth of field.

Each nanoparticle Pd and Ru on surfaces rGO has a uniform, compact morphology and is homogenously distributed on surface rGO (Zadora and Brożek-Mucha, 2003). In this study, according to SEM characterization as we know the structure Pd@Ru/rGO appeared that all Pd and Ru coated in different working areas/different magnifications (Figure 4.1) 1 nm/20.00 KX, 200 nm/100 KX, 100 nm/200 KX.

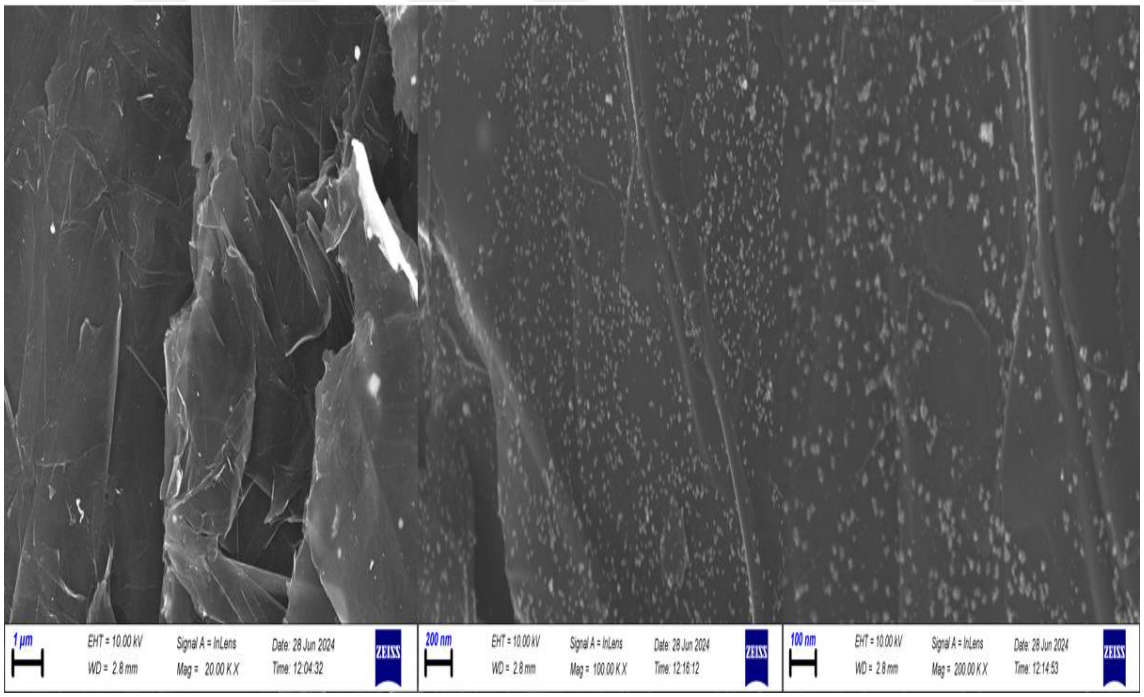

Figure 4.1 SEM image of Pd@Ru/ rGO from low magnification into high magnifications

Another examination is a result of EDX analysis that is in the working area 0.2 um micrometer that was obtained, and each color represents the distribution of elements in Pd@Ru/rGO on the other hand the yellow dots are carbon atoms (C) and the green dots are ruthenium (Ru) atoms, the red dots are oxygen (O) atoms, the purple dots are palladium (Pd) atoms. Then we can say these two elements palladium (Pd) and ruthenium (Ru) are homogeneously distributed on the surface rGO (Figure 4.2.).

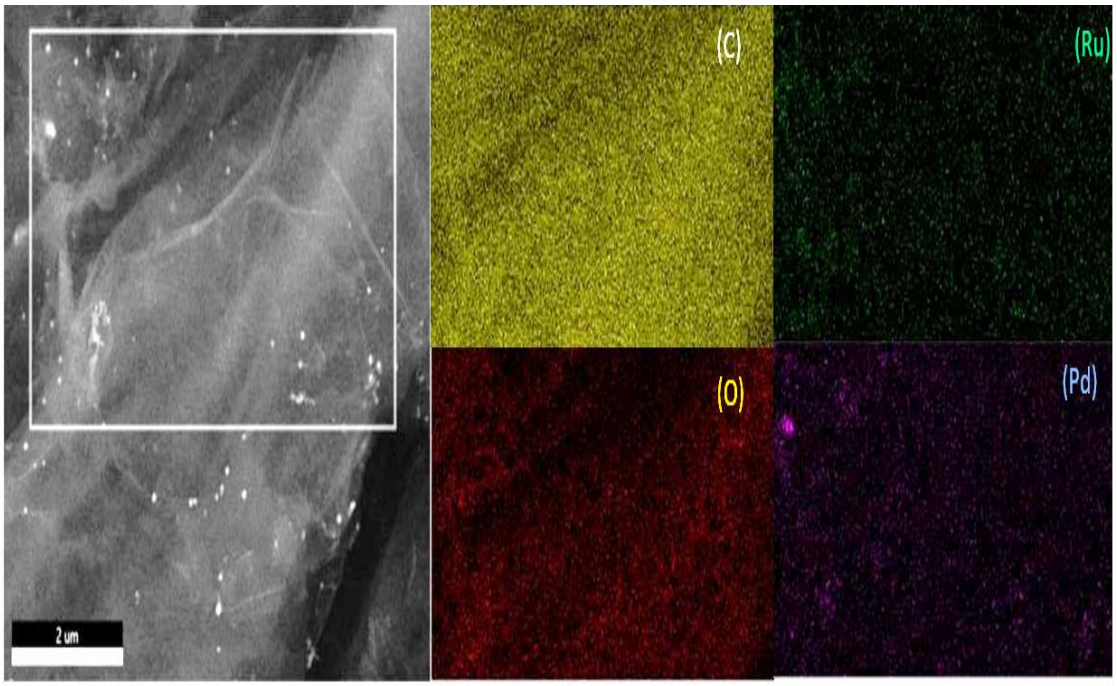

Figure 4.2 EDX mapping image 1 um of Pd@Ru/rGO

4.2 XRD Results

X-ray diffraction is an analytical method that depends on the diffraction of x-rays by matter, especially crystalline substances, x-ray diffraction is an elastic scattering process that results in enhanced interference as increasingly ordered materials are examined, without any loss of photon energy. For nanocrystalline materials, the term "diffusion" is more appropriate. This is an effective nondestructive method for characterizing crystalline materials, providing thoughts into structures, phases, preferred crystal orientations, and other structural parameters, including average grain size, crystallinity, stress, and crystal defects. This method is critically significant in the fields of science, engineering, and technology (El Bourakadi et al., 2021a).

XRD is a device to correctly detect the structure and composition, like crystallography and detection of each peak related to the material in the structure components, meaning that each packs XRD that show in the pattern increased or decreased due to the morphology of the crystals (El Bourakadi et al., 2021b). In this study during the examination of XRD the rGO used is commercial and it is amorphous also with a large amount of crystallinity hexagonal structure the ratio between 0 to 40 theta degrees indicates that carbon and graphite.

The examination of XRD indicates that the palladium (Pd) 2θ = 40°, and ruthenium (Ru) 2θ =43°, mention at (Figure 4.3) (Zhang et al., 2017; Boukhoubza et al., 2019). Some peaks have a higher intensity than others in (Figure 4.3) this is because of the crystal's orientations. When we investigated the rGO pattern and Pd@Ru/rGO, each element Pd and Ru were fixed on the surface rGO and produced (W. Li et al., 2016; Q. He et al., 2020).

As a result, compounds with good crystallinity are produced. XRD is a flexible, non-destructive analytical method for examining solid, powder, or liquid samples' phase composition, crystal structure, and orientation. Due to the XRD examination, the red peak is pd@Ru/rGO examinations and the black one is only rGO examination shows in Figure 4.3 that we can see a palladium peak is (111) degrees and the carbon peak (002) degrees the black pattern only rGO (Figure 4.3).

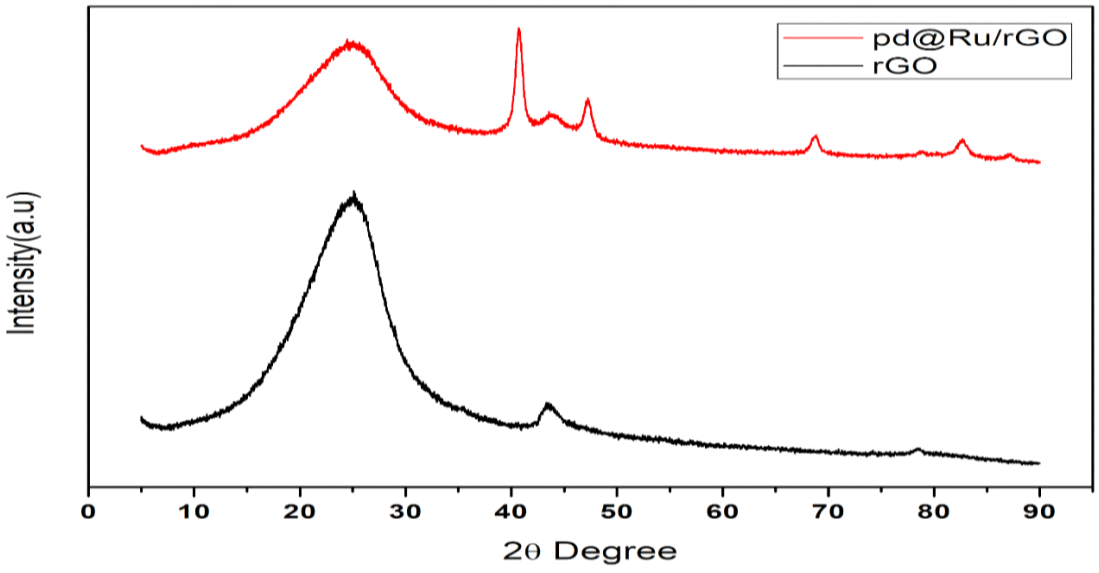

Figure 4.3 XRD patterns: The red one is Pd@Ru/rGO, and the black one is rGO

4.3 XPS Results

Determines the surface's elemental composition by XPS. This method involves examining the emitted photoelectrons after x-ray irradiation of the sample. XPS, unlike EDX, only analyzes the surface elemental composition because of its shallow depth profile of less than 10 nm (Cornu et al., 2023). During XPS examinations, we observed that Pd and Ru are coated into the surface rGO due to the binding energy and peak observed (Figure 4.4).

The XPS spectrum of palladium exhibits two peaks, two peaks at 335.1 ev and 340.4 ev, and binding energies corresponding to (Pd) 3d5/2 and (Pd) 3d3/2, respectively (Yang et al., 2014). That means that Pd is coated on the surface. rGO also has different binding energy (oxidation state), similar to this study, as approved in (Figure 4.4); three peaks at 285.4 ev, 286.9 ev, and 289.4 ev are attributed to sp3 bulk bonded carbon C-C, C-O chemical bonds, and C=O bonds appeared, according to the structure of rGO C_1s are bulky bonded in hybridization sp^3 (Dolgov et al., 2015).

XPS image analyzes Ru_3d = 284 ev binding energy in (Figure 4.3), indicating the similar ratio Ru_3d = 284 ev binding energy (Papaderakis et al., 2014). The atomic percentage of each C_1s %80.7, O_1s %13.6, Ru_3d %4.7, Na_1s %0.8, Pd_3d %0.2. In conclusion, XPS aims to investigate a material's chemical state and elemental composition. The oxidation state from the ground state into the excited state is between (0 to 2+) for each NP of Pd and Ru coated on the surface rGO.

Table 4.1 According to pattern Figure 4.4, each element has the top percentage ratio of atomics

Atomic	%
C_1s	80. 7
O_1s	13. 6
Ru_3d	4. 7
Na_1s	0. 8
Pd_3d	0.2

The blue color is a wide scanning xps Pd@Ru/rGO according to (Figure 4.4) Pd on the surface rGO appears at spectrum 330 - 360 ev that, then Ru binding energy appears at

region 280-330 ev its green color, GO (C_1s) peak position (284 - 286) ev binding energy appears, the peak represent as (O_1s) that occur at binding energy ratio (530 - 533) ev, each peak is represented by the shell of elements, so according to these data we can discuss it and approve it by references.

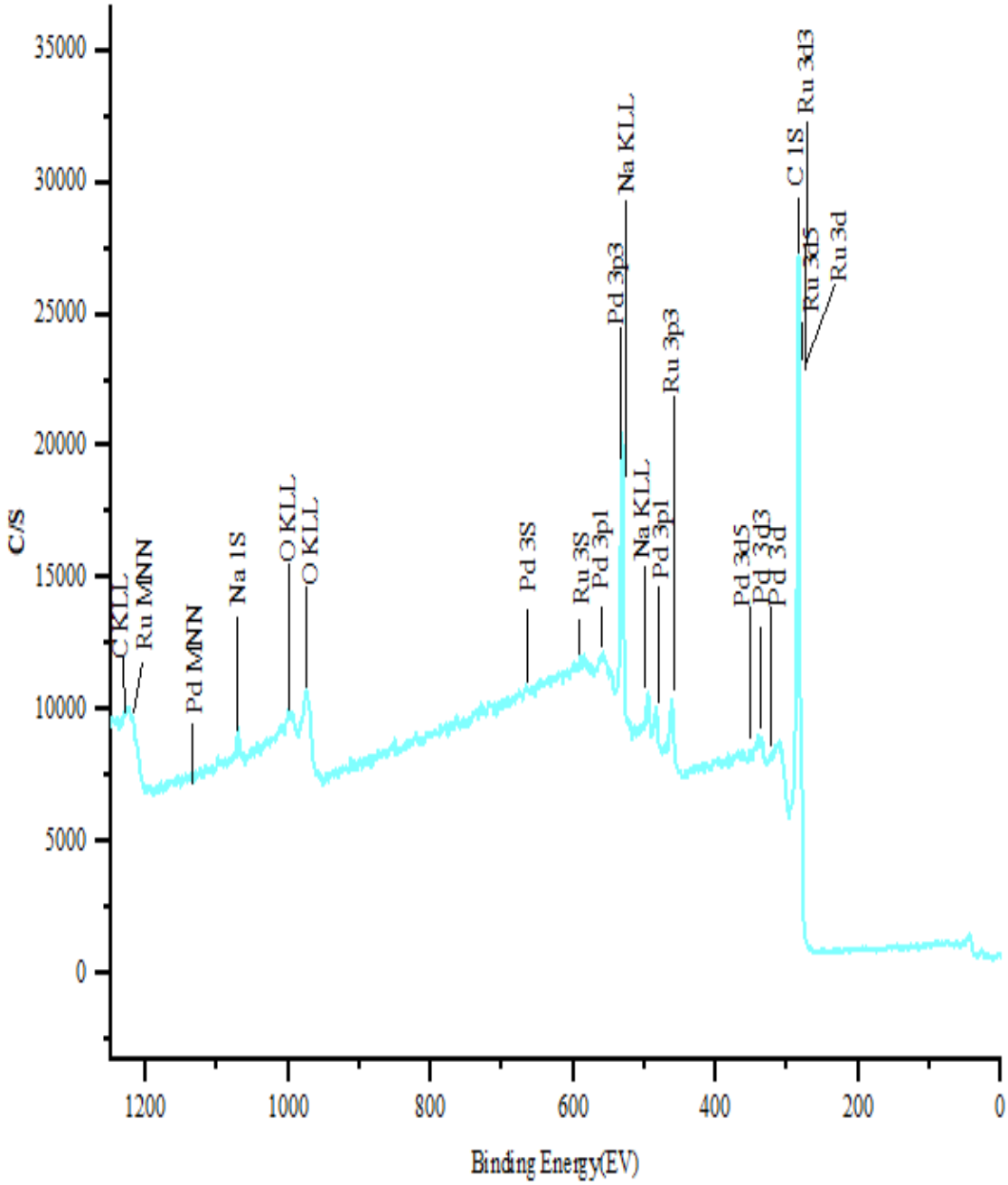

Figure 4.4 Broad survey range scan spectrum of XPS Pd@Ru/ rGO

4.4 Electrochemistry Results

Before modifying the working electrode, (GCE) was polished using alumina slurry and cleaned with a nitric acid/water (1:1) solution and ethanol for 5 minutes. Respectively, an ultrasonic bath was employed until a reflective surface of GCE was attained. To achieve a 1.0 mg/mL dispersion, 1 mg of Ru/Pd/rGO/GCE was added to 1 mL of ultrapure water and sonicated until a homogeneous mixture was attained. Subsequently, 5 µL of the dispersion was applied to the GCE and dried in a vacuum oven at 50 °C. The remaining electrodes utilized in the study were fabricated following the previously outlined procedure.

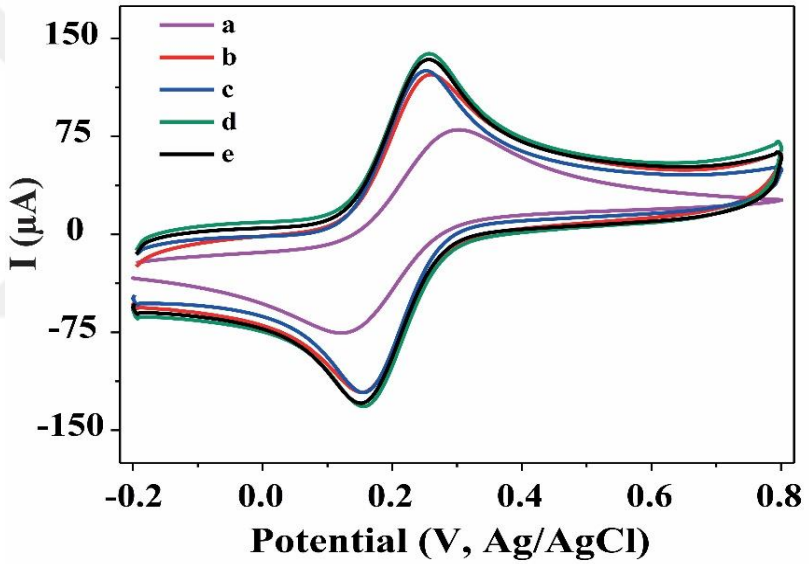

Figure 4.5 Cyclic voltammograms of (a) GCE, (b) rGO/GCE, (c) Pd/rGO/GCE, (d) Ru/rGO/GCE, and Ru/Pd/rGO/GCE obtained in 5 mM $[Fe(CN)_6]^{3-}$/ $[Fe(CN)_6]^{4-}$ containing 0.1 M KCl at 0.05 V/s

Figure 4.5 Displays the cyclic voltammograms of the redox probe obtained at the moderated electrodes. The anodic peak current values of the probe were recorded 79.18 µA on GCE (Figure 4.5a), 105.66 µA on rGO/GCE (Figure 4.5b), 111.84 µA on Pd/rGO/GCE (Figure 4.5c), 113.28 µA on Ru/rGO/GCE (Figure 4.5d), and 113.41 µA on Ru/Pd/rGO/GCE (Figure 4.5e). These results demonstrate that Ru/Pd/rGO/GCE exhibited the highest oxidation peak current at the scan rate of 0.05 V/s.

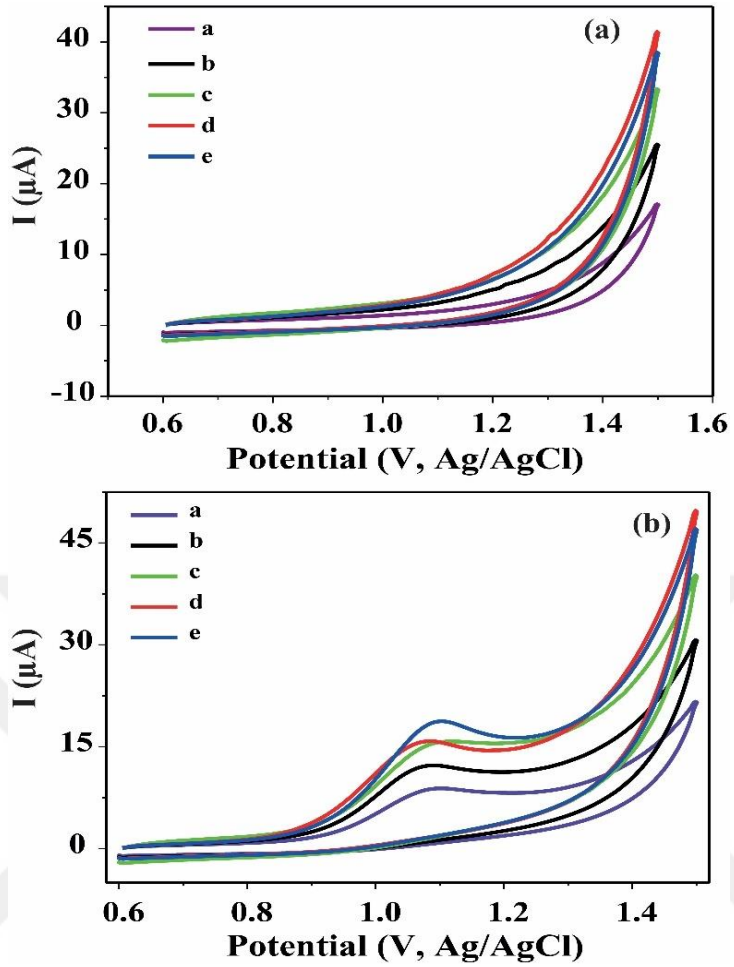

Figure 4.6 (a) Cyclic voltammograms of (a) GCE, (b) rGO/GCE, (c) Pd/rGO/GCE, (d) Ru/rGO/GCE, and Ru/Pd/rGO/GCE obtained in BR buffer (pH 5.0) in the absence (a) and presence of 0.1 mM ENR (b)

Cyclic voltammetry was conducted to evaluate the electrochemical response of the modified electrodes to enrofloxacin (ENR) (Figure 4.6) The anodic peak current value of 0.1 mM of ENR was 3.70 µA on GCE (Figure 4.6 ba), 5.14 µA on rGO/GCE (Figure 4, 6 bb), 6.12 µA on Pd/rGO/GCE (Figure 4.6 bc), 6.29 µA on Ru/rGO/GCE (Figure 4.6 bd), and 8.35 µA on Ru/Pd/rGO/GCE (Figure 4.6 be) at a scan rate of 50 mV/s. The voltammograms show that the maximum anodic peak current was achieved on the Ru/Pd/rGO/GCE working electrode.

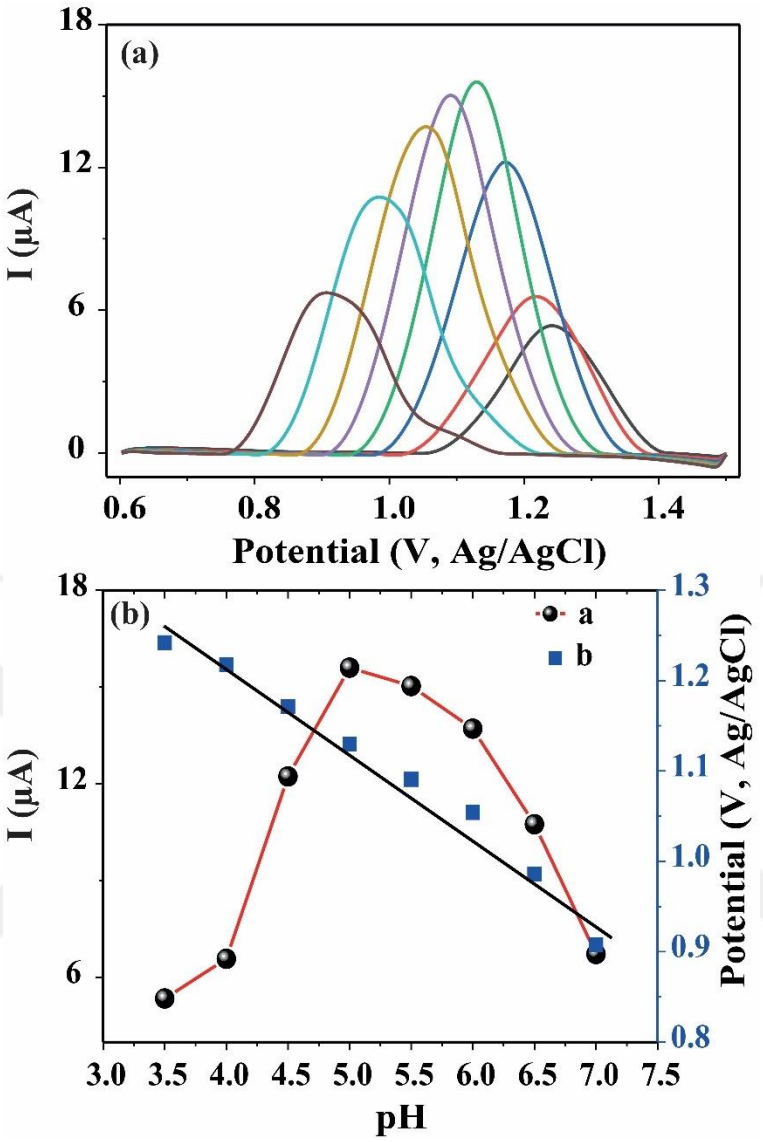

Figure 4.7 (a) Linear sweep voltammograms of Ru/Pd/rGO/GCE obtained in BR buffer with various pH values (3.5-7.0) in the presence of ENR (b) current versus pH graph and potential versus pH graph

The pH of the employed buffer solution is a critical parameter in the electrochemical reaction .In the present study, Britton-Robinson buffer solution (BR) with a pH scale ranging from 3.5 to 7.0 was performed. Figure 4.7a presents cyclic voltammograms acquired in BR buffer solution at unlikely pH levels. The anodic peak current of ENR rises with the increasing pH of the electrolyte (from 3.5 to 5.0) and subsequently declines as pH increases (from 5.0 to 7.0). Consequently, a BR buffer solution with a pH of 5.0 was employed in all electrochemical experiments. The equation for linear regression can be written as follows (Figure 4.7b): Epc (mV) = − 0.0927pH +

1.5863 (R^2= 0.977). The ratio of m/n was computed to be 1.56 using the Nernst equation (Zhao et al., 2015) as expressed below (4.1).

$$Epc = E^{\theta} - [(2.303mRT)/(nF)]\ pH \quad (4.1)$$

Where m indicates the number of protons involved in the reduction process, n represents a transfer electrons number, and R, T, and F have the standard definitions. This result indicates that the proton transfer number could be computed if the number of transfer electrons was obtained.

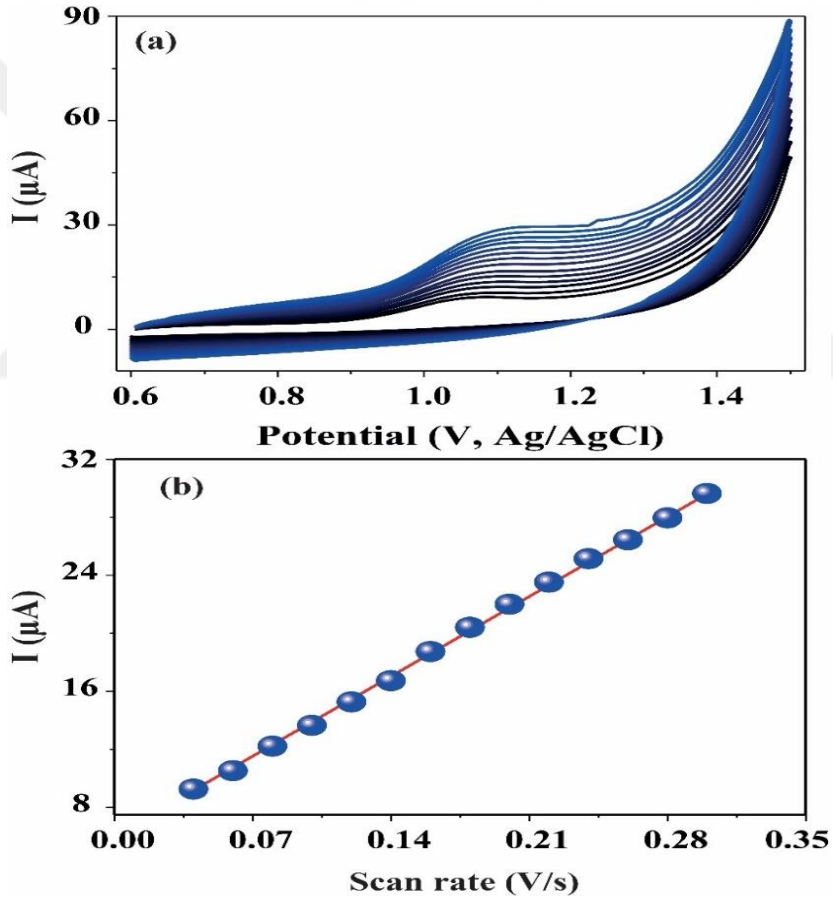

Figure 4.8 (a) Cyclic voltammograms obtained on Ru/Pd/rGO/GCE in BR buffer (pH 5.0) containing ENR at various scan rates (from 0.04 to 0.30 V/s) (b) current versus scan rate graph

To examine the impact of scan rate on the electrochemical response of Ru/Pd/rGO/GCE (Huang et al., 2020) to ENR, CVs were recorded in BR buffer (pH 5.0)

containing ENR at various scan rates (Figure 4.8a). The voltammograms demonstrate that the anodic peak current values consistently increased with the rise in scan rate from 0.04 to 0.3 V/s. The linear relationship between anodic peak current and scan rate (Figure 4.8b) indicates a characteristic adsorption-controlled electrode process for the electrocatalytic reaction of ENR on Ru/Pd/rGO/GCE (Huang et al., 2020). The linear regression equations were (4.2):

$$I_{pa}(\mu A) = 79.491\nu(V/s) + 5.8901 \text{ with } R^2 = 0.9993 \quad (4.2)$$

The fabricated Ru/Pd/rGO/GCE working electrode was utilized for the electrochemical assessment of ENR using differential pulse voltammetry (DPV). Before obtaining the linear graph, optimum values such as deposition potential and deposition time were determined. The sensor response was recorded as ENR was incrementally introduced to the electrochemical cell containing N2-saturated BR buffer at pH 5.0.

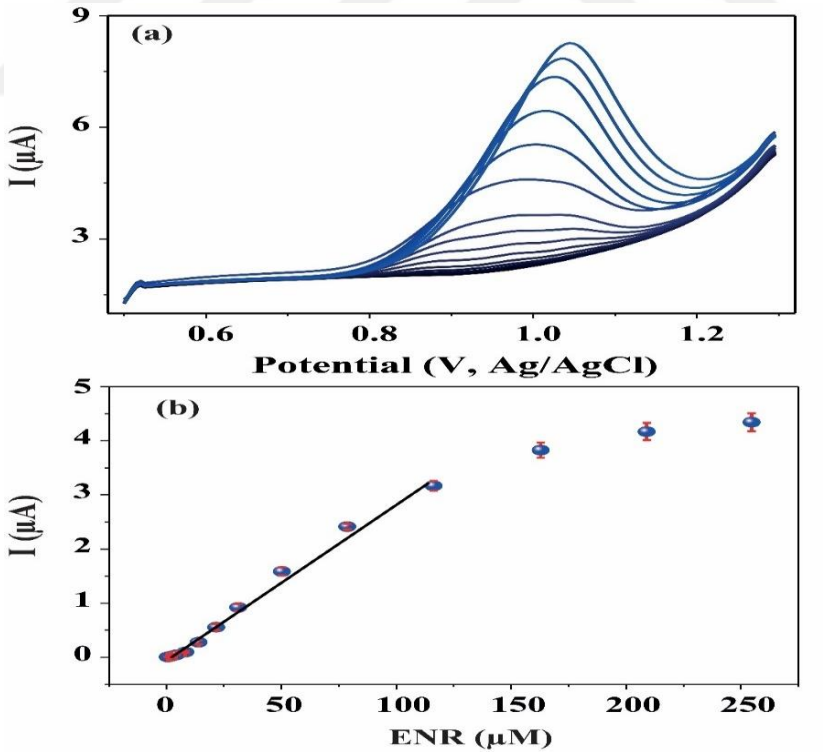

Figure 4.9 (a) Differential pulse voltammetric response of Ru/Pd/rGO/GCE in BR buffer (pH 5.0) to ENR (b) current versus concentration of ENR graph (deposition potential: 0.5V, deposition time: 90 s, scan rate: 0.01 V/s, modulation amplitude: 0.025 V, modulation time: 0.05 s)

The sensor response was recorded as ENR was incrementally introduced to the electrochemical cell containing N2-saturated BR buffer at pH 5.0. Figure 4.9a illustrates a graph of current versus potential. The working electrode exhibited a dynamic linear range for the determination of ENR. The linear range was determined to be between 0.6 and 116 µM. (Figure 4.9b) The regression equations were (4.3).

$$I(\mu A) = 0.0291C(\mu M) - 0.0415 \ (R^2 = 0.991) \quad (4.3)$$

The sensor's detection limit (LOD) was calculated to be 0.2 µM depending on signal-to-noise ratio of 3(S/N = 3).

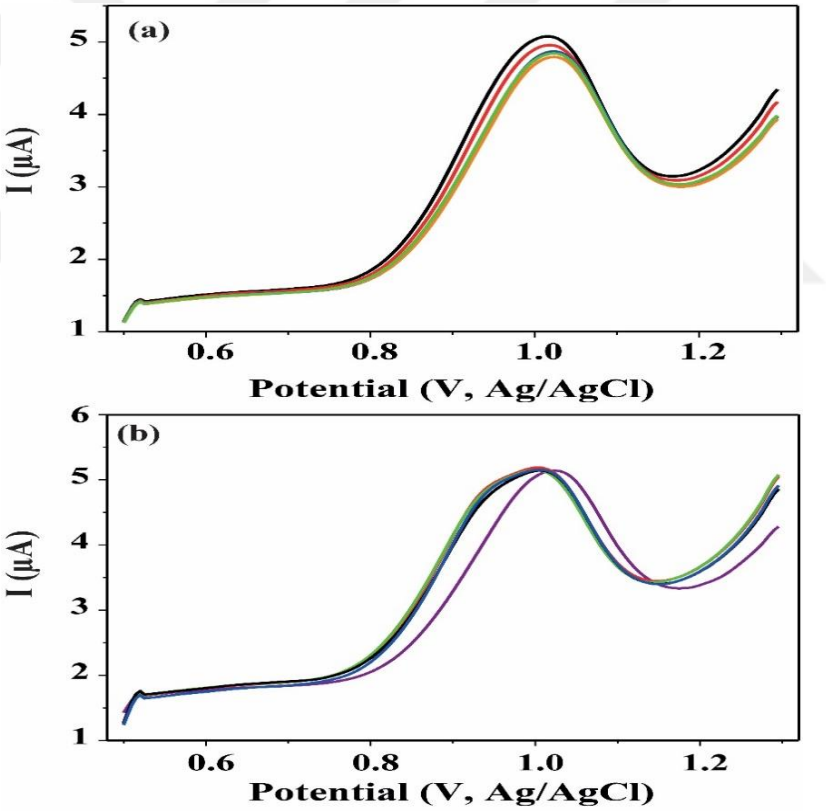

Figure 4.10 (a) Repeatability and (b) reproducibility results of Ru/Pd/rGO/GCE

Some organic and inorganic species disturb the Ru/Pd/rGO/GCE sensor response to ENR, which was evaluated using amperometry. Some substances we are used to ion selectivity such as 500-fold of 0.1 mM Na^+, 0.1 mM Cl^-, 0.1 mM glucose, 0.1 mM glycin,

0.005 mM dopamine, 0.025 mM paracetamol, 0.1 mM ascorbic acid, and 0.1 mM pyrocatechol, 0.1 mM, K^+, 0.025 mM uric acid displayed limited affect the analyte signal, with deviations under 2.0%. The outcomes of the selectivity tests indicated that the sensor is appropriate for determining ENR.

The study utilized 73.89 µM of ENR to assess the repeatability of the Ru/Pd/rGO/GCE sensor. Measurements were acquired using the DPV method. To this purpose, five measurements were conducted for 73.89 µM of ENR utilizing the same Ru/Pd/rGO/GCE sensor fabricated under similar conditions. The standard deviation (SD) and relative standard deviation (RSD) were determined to be 0.073 and 3%, respectively. (Figure 4.10a). Five Ru/Pd/rGO/GCE sensors were fabricated under identical conditions in the reproducibility study. The current-potential graph was generated using 73.89 µM of ENR, as in the repeatability study. The standard deviation (SD) and relative standard deviation (RSD) were 0.037 and 1.38%, respectively (Figure 4.10b). The results indicated that the sensor demonstrated adequate repeatability and reproducibility. The sensor's 30-day storage stability was examined. The sensor exhibited a 95.42% response to the analyte on the 30th day, indicating satisfactory stability.

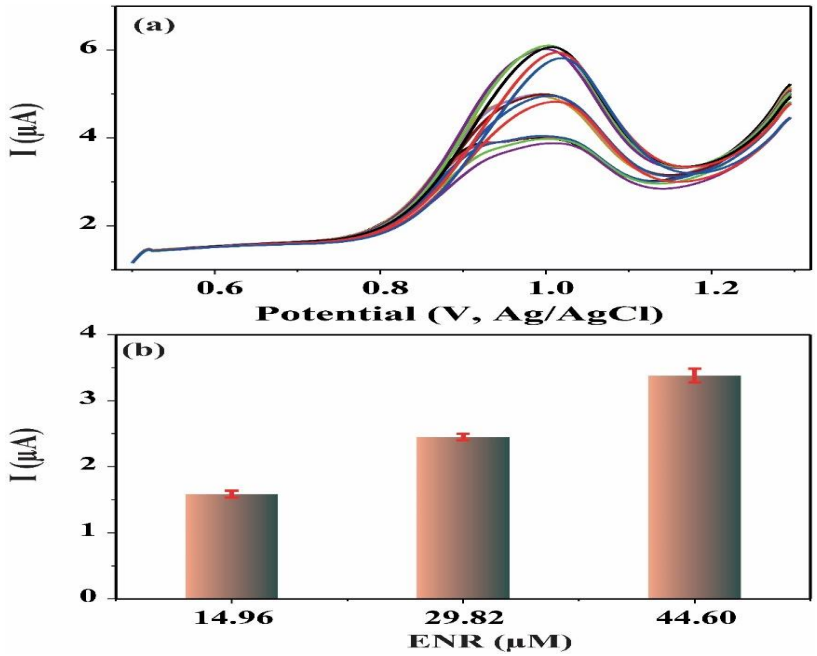

Figure 4.11 (a) Differential pulse voltammetric results of ENR were obtained on Ru/Pd/rGO/GCE electrochemical sensor (b) current versus the concentrations used in the ENR graph

The Ru/Pd/rGO-modified GCE was subsequently employed to quantify ENR in a table form. Various concentrations of ENR were prepared in ultrapure water, and differential pulse voltammetry measurements for the electrooxidation of ENR were conducted. Figures 4.11a and 4.11b illustrate that outstanding electrochemical responses were obtained in the actual samples, as detailed in Table 4.2. The recoveries achieved for ENR in the samples ranged from 93.63% to 103.88%. I demonstrated that the Ru/Pd/rGO/GCE electrochemical sensor is a reliable instrument for experimental studies.

Table 4.2 Detection of ENR in ENR containing tables

Samples	Added (µM)	Found (µM)	RSD (%)	Recovery (%)
1	14. 96	15. 54 ± 0 . 51	2 . 65	103. 88
2	29. 82	29. 44 ± 0 . 6	1 . 51	98. 73
3	44. 60	41. 76 ± 1 . 29	2 . 49	93. 63

5. DISCUSSION AND CONCLUSION

In this study, synthesized pd@Ru/rGO glassy carbon electrode to detect enrofloxacin that was antibacterial and had great importance in animal and human health, palladium (Pd) and ruthenium nanoparticles (Ru) was coated on the surface reduced graphene oxide, and after preparation of Pd@Ru/rGO, it is examined by scanning an electron microscope (SEM); as a result, we were obtained each nanoparticle Pd and Ru on surfaces rGO has a uniform, compact morphology and each nanoparticle are homogenously distributed on surface rGO, due to different magnifications with different working areas (Figure 4.1).

SEM analysis of Pd@Ru/ rGO showed that the Pd and Ru nanoparticles were homogeneity and distribution into reduced graphene oxide surfaces from low magnifications to high magnifications. magnification starts from; 20.00 KX , 1 00.00 KX , 200.00 KX with different nanometers sequence 1micrometer, 200 nm, 100nm. SEM and EDX devices deal with morphology and surface analysis (Zadora and Brożek-Mucha, 2003). Then, EDX devices detected palladium and ruthenium's regular dispersion on the surface rGO, which appears uniform (Figure 4.2).

Another surface analysis, XRD, was an efficient nondestructive technique for characterizing crystalline materials. XRD obtains information about structures, phases, and preferred crystal orientations. The XRD method is critically significant in science, engineering, and technology (El Bourakadi et al., 2021a). An XRD device was used to detect each nanoparticle element on the surface rGO coated and determine the crystallinity and purity of the samples (El Bourakadi et al., 2021b). In this study, we observed that the palladium Pd peak appeared at $2\theta = 40°$, and the ruthenium Ru peak appeared at $2\theta = 43°$, in (Figure 4.3), which is also similar to the literature review (Zhang et al., 2017; Boukhoubza et al., 2019) . Some peaks were more intense than others because of the crystal's orientations; in (Figure 4.3) when we investigate the rGO pattern and Pd@Ru/rGO, we know each element, Pd and Ru, was fixed on the surface rGO and produced Pd@Ru/rGO (W. Li et al., 2016; Q. He et al., 2020).

XPS device in this study was used to ascertain the elemental composition of the surface analysis Pd@Ru/rGO characterized by XPS and also to detect and determine the oxidation state of each nanoparticles palladium and ruthenium were used as nanoparticles

and have oxidation state (0 to +2) between ground stated into an excited state when bombarded by energy level. Also, each was detected and appeared in the (Figure 4.4) survey analysis. Each nanoparticle had a different binding energy and was similar in oxidation state +2. The XPS spectrum of palladium exhibits two peaks, at 335.1 ev and 340.4 ev, binding energies corresponding to Pd 3d5/2 and Pd 3d3/2, respectively (Yang et al., 2014). That means that Pd was coated on the surface rGO, which also has different binding energies, similar to this study (Figure 4.4). Three peaks at 285.4 ev, 286.9 ev, and 289.4 ev, are attributed to sp3 bulk bonded carbon C-C, C-O chemical bonds, and C=O bonds appeared in (Figure 4.4) according to the structure of rGO, C1s bulky bonded in sp3 (Dolgov et al., 2015).

XPS image analyzes Ru3d = 284 ev binding energy in (Figure 4.3) indicating also the similar ratio Ru3d = 284 ev binding energy (Papaderakis et al., 2014). Generally, according to SEM and EDX, XRD and XPS were used to surface analyze the characterization of Pd@Ru/rGO. We know that successfully synthesized was ready to prepare an electrochemical sensor to detect enrofloxacin.

Table 5.1 presents the outcomes achieved for ENR utilizing diversely modified electrodes. In comparison to previously reported studies, the fabricated Ru/Pd/rGO/GCE sensor exhibited a broad linear determination range and high sensitivity with a low limit of detection, highlighting the significant synergistic effect between reduced graphene oxide, palladium, and ruthenium nanoparticles, therefore if compare to MIP electrochemical in this work electrodes better than some MIP electrodes to detection enrofloxacin due to (Table 5.1) that by references approve it, but if compare to novel electrochemical sensors some electrochemical sensors are better than observed electrochemical sensor to detect enrofloxacin according to high repeatability, high reproducibility, high stability, and sensitivity observed electrode is better than any other electrodes that in the table that approved by references, therefore, we can suggested that this electrode Pd@Ru/rGO/GCE was successfully synthesis to detection enrofloxacin.

In conclusion, ENR was determined using the Ru/Pd/rGO/GCE sensor fabricated in this study. The sensor showed a satisfactory linear detection range from 0.6 to 116 µM. LOD value was determined as 0.2 µM based on S/N = 3. Also, the sensitivity of the electrode is 0.0291 $\mu A\,\mu M$. The sensor showed excellent selectivity towards the electroactive compounds used. It demonstrated excellent repeatability and reproducibility

according to the obtained standard deviation, relative standard deviation, and recoveries. Considering these results, the prepared Ru/Pd/rGO material exhibited satisfactory results.

Table 5.1 This table compares this study and reviews each paper due to the linear range, LOD, and peak potential reported in this table

Electrode materials	Linear range µM	LOD µM	Peak potential (V)s	References
Pd@Ru/ rGO/GCE	0.6 - 116	0. 2	0. 05	this work
MWCNTs/MIPS/GCE	2.8×10^{-5} - 28	0. 9	0. 2	(Chen et al., 2022c)
$CaWO_4$ / RGO (CW / RGO)	0.001 - 115	0.021	0. 05	(Karuppusamy et al., 2022)
CoCH - 6 h / GCE	0.5 - 65	0. 1	1. 15	(Yu et al., 2024)
TAPB- PDA - COFs / Au NPs	0.05- 10 10- 120	0. 04	0. 1	(S. Lu et al., 2021)
rCNT/GCE	0. 005-0. 05 0.05 – 1.5	0.002	0. 3	(Doan et al., 2024)

Future prospects:

Due to the fabrication of a new novel electrochemical sensor Pd@Ru/rGO. It is possible to use another platinum group or transition metal nanoparticles instead of palladium and ruthenium to fabricate new electrodes to detect any other antibiotic in tablet or serum due to the condition of the fabrication electrodes sensor and response to the electrochemical sensor. The most important is that its generation of new electrodes may be an error. However, it can increase the ability of electrodes due to changes in the condition of each parameter used in this paper.

REFERENCES

Abd El-Hady, M. N., Gomaa, E. A., Al-Harazie, A. G. (2019). Cyclic voltammetry of bulk and nano CdCl2 with ceftazidime drug and some DFT calculations. *Journal of Molecular Liquids*, 276, 970–985. doi:10.1016/j.molliq.2018.10.125

Adams, B. D., Chen, A. (2011). The role of palladium in a hydrogen economy. *Materials Today*, 14(6), 282–289. doi:10.1016/S1369-7021(11)70143-2

Al-Harazie, A. G., Gomaa, E. A., Zaky, R. R., Abd El-Hady, M. N. (2024). Cyclic voltammetry studies of malonamide hydrazone derivative and its electrochemical effect on CdCl2. *Electrochimica Acta*, 476, 143690. doi:10.1016/j.electacta.2023.143690

Antolini, E. (2009). Palladium in fuel cell catalysis. *Energy & Environmental Science*, 2(9), 915. doi:10.1039/b820837a

Baldwin, R. P., Christensen, J. Kai., Kryger, Lars. (1986). Voltammetric determination of traces of nickel(II) at a chemically modified electrode based on dimethylglyoxime-containing carbon paste. *Analytical Chemistry*, 58(8), 1790–1798. doi:10.1021/ac00121a042

Boukhoubza, I., Khenfouch, M., Achehboune, M., Mothudi, B. M., Zorkani, I., Jorio, A. (2019). X-ray diffraction investigations of nanostructured ZnO coated with reduced graphene oxide. *Journal of Physics: Conference Series*, 1292(1), 012011. doi:10.1088/1742-6596/1292/1/012011

Canales, C., Peralta, E., Antilen, M. (2019). Electrochemical techniques to detect and quantify Enrofloxacin in presence of highly potential interferences: Assays in Chilean aqueous-soil matrices. *Journal of Electroanalytical Chemistry*, 832, 329–335. doi:10.1016/j.jelechem.2018.10.064

Chen, J., Tan, L., Qu, K., Cui, Z., Wang, J. (2022a). Novel electrochemical sensor modified with molecularly imprinted polymers for determination of enrofloxacin in marine environment. *Microchimica Acta*, 189(3), 95. doi:10.1007/s00604-022-05205-9

Chen, J., Tan, L., Qu, K., Cui, Z., Wang, J. (2022b). Novel electrochemical sensor modified with molecularly imprinted polymers for determination of enrofloxacin in marine environment. *Microchimica Acta*, 189(3), 95. doi:10.1007/s00604-022-05205-9

Chen, J., Tan, L., Qu, K., Cui, Z., Wang, J. (2022c). Novel electrochemical sensor modified with molecularly imprinted polymers for determination of enrofloxacin in marine environment. *Microchimica Acta*, 189(3), 95. doi:10.1007/s00604-022-05205-9

Chuah, S., Pan, Z., Sanjayan, J. G., Wang, C. M., Duan, W. H. (2014). Nano reinforced cement and concrete composites and new perspective from graphene oxide. *Construction and Building Materials*, 73, 113–124. doi:10.1016/j.conbuildmat.2014.09.040

Clarke, M. J. (2003). Ruthenium metallopharmaceuticals. *Coordination Chemistry Reviews*, 236(1–2), 209–233. doi:10.1016/S0010-8545(02)00312-0

Cornu, R., Laurent, G., Beduneau, A. (2023). Preparation and characterization of PLGA nanoparticles. *Poly(lactic-co-glycolic acid) (PLGA) Nanoparticles for Drug Delivery* (pp. 27–54). Elsevier. doi:10.1016/B978-0-323-91215-0.00012-1

Cui, L., Lin, X., Lin, N., Song, Y., Zhu, Z., Chen, X., Yang, C. J. (2012). Graphene oxide-protected DNA probes for multiplex microRNA analysis in complex biological

samples based on a cyclic enzymatic amplification method. *Journal of Chemical Comunications.*, 48 (2), 194–196. doi:10.1039/C1CC15412E

Doan, T. D., Pham, Y. T. H., Nhung, H. T., Oanh, H. T., Duc, T. N., Le, H. Q., … Hoang, M. H. (2024). Fabrication and application of functionalized carbon nanotubes for highly sensitive and selective sensing of enrofloxacin. *Vietnam Journal of Chemistry*, 62(S1), 76–85. doi:10.1002/vjch.202300298

Dolgov, A., Lopaev, D., Lee, C. J., Zoethout, E., Medvedev, V., Yakushev, O., Bijkerk, F. (2015). Characterization of carbon contamination under ion and hot atom bombardment in a tin-plasma extreme ultraviolet light source. *Applied Surface Science*, 353, 708–713. doi:10.1016/j.apsusc.2015.06.079

El Bourakadi, K., Bouhfid, R., Qaiss, A. el K. (2021a). Characterization techniques for hybrid nanocomposites based on cellulose nanocrystals/nanofibrils and nanoparticles. *Cellulose Nanocrystal/Nanoparticles Hybrid Nanocomposites* (pp. 27–64). Elsevier. doi:10.1016/B978-0-12-822906-4.00010-4

El Bourakadi, K., Bouhfid, R., Qaiss, A. el K. (2021b). Characterization techniques for hybrid nanocomposites based on cellulose nanocrystals/nanofibrils and nanoparticles. *Cellulose Nanocrystal/Nanoparticles Hybrid Nanocomposites* (pp. 27–64). Elsevier. doi:10.1016/B978-0-12-822906-4.00010-4

El Gindy, A. A., Gomaa, E. A., Abdelkader, H. I., Mohsen, A., Habib, A. O. (2022). The effect of a sulfonated naphthalene-based polymer on redox reaction data, potassium ferrocyanide complexation, and the compressive strength of Portland cement paste. *Journal of Molecular Liquids*, 356, 119000. doi:10.1016/j.molliq.2022.119000

Elgrishi, N., Rountree, K. J., McCarthy, B. D., Rountree, E. S., Eisenhart, T. T., Dempsey, J. L. (2018). A Practical Beginner's Guide to Cyclic Voltammetry. *Journal of Chemical Education*, 95(2), 197–206. doi:10.1021/acs.jchemed.7b00361

Favier, I., Pla, D., Gómez, M. (2020). Palladium Nanoparticles in Polyols: Synthesis, Catalytic Couplings, and Hydrogenations. *Chemical Reviews*, 120(2), 1146–1183. doi:10.1021/acs.chemrev.9b00204

Gallegos-Tabanico, A., Jimenez-Canale, J., Hernandez-Leon, S. G., Burgara-Estrella, A. J., Encinas-Encinas, J. C., Sarabia-Sainz, J. A. (2022). Development of an Electrochemical Sensor Conjugated with Molecularly Imprinted Polymers for the Detection of Enrofloxacin. *Chemosensors*, 10(11), 448. doi:10.3390/chemosensors10110448

Grabowski, Ł., Gaffke, L., Pierzynowska, K., Cyske, Z., Choszcz, M., Węgrzyn, G., Węgrzyn, A. (2022). Enrofloxacin—The Ruthless Killer of Eukaryotic Cells or the Last Hope in the Fight against Bacterial Infections?. *International Journal of Molecular Sciences*, 23(7), 3648. doi:10.3390/ijms23073648

He, Q., Ji, J., Zhang, Q., Yang, X., Lin, Y., Meng, Q., … Xu, M. (2020). PdMn and PdFe nanoparticles over a reduced graphene oxide carrier for methanol electro-oxidation under alkaline conditions. *Ionics*, 26(5), 2421–2433. doi:10.1007/s11581-019-03343-4

He, S., Song, B., Li, D., Zhu, C., Qi, W., Wen, Y., … Fan, C. (2010). A Graphene Nanoprobe for Rapid, Sensitive, and Multicolor Fluorescent DNA Analysis. *Advanced Functional Materials*, 20(3), 453–459. doi:10.1002/adfm.200901639

Heck, R. F., Nolley, J. P. (1972). Palladium-catalyzed vinylic hydrogen substitution reactions with aryl, benzyl, and styryl halides. *The Journal of Organic Chemistry*, 37(14), 2320–2322. doi:10.1021/jo00979a024

Huang, Q., Lin, X., Tong, L., Tong, Q.-X. (2020). Graphene Quantum Dots/Multiwalled Carbon Nanotubes Composite-Based Electrochemical Sensor for Detecting Dopamine Release from Living Cells. *ACS Sustainable Chemistry & Engineering*, 8(3), 1644–1650. doi:10.1021/acssuschemeng.9b06623

Karuppusamy, N., Mariyappan, V., Chen, S.-M., Ramachandran, R. (2022). A novel electrochemical sensor for the detection of enrofloxacin based on a 3D flower-like metal tungstate-incorporated reduced graphene oxide nanocomposite. *Nanoscale*, 14(4), 1250–1263. doi:10.1039/D1NR06343J

Kohanski, M. A., Dwyer, D. J., Collins, J. J. (2010). How antibiotics kill bacteria: from targets to networks. *Nature Reviews Microbiology*, 8(6), 423–435. doi:10.1038/nrmicro2333

Kumar, V., Kumar, A., Lee, D.-J., Park, S.-S. (2021). Estimation of Number of Graphene Layers Using Different Methods: A Focused Review. *Materials*, 14(16), 4590. doi:10.3390/ma14164590

Kwon, H., Mondal, J., AlOgab, K. A., Sammelselg, V., Takamichi, M., Kawaski, A., Leparoux, M. (2017). Graphene oxide-reinforced aluminum alloy matrix composite materials fabricated by powder metallurgy. *Journal of Alloys and Compounds*, 698, 807–813. doi:10.1016/j.jallcom.2016.12.179

Ławkowska, K., Pokrywczyńska, M., Koper, K., Kluth, L. A., Drewa, T., Adamowicz, J. (2021). Application of Graphene in Tissue Engineering of the Nervous System. *International Journal of Molecular Sciences*, 23(1), 33. doi:10.3390/ijms23010033

Lerf, A., He, H., Forster, M., Klinowski, J. (1998). Structure of Graphite Oxide Revisited. *The Journal of Physical Chemistry B*, 102(23), 4477–4482. doi:10.1021/jp9731821

Li, F., Jiang, X., Zhao, J., Zhang, S. (2015). Graphene oxide: A promising nanomaterial for energy and environmental applications. *Nano Energy*, 16, 488–515. doi:10.1016/j.nanoen.2015.07.014

Li, W., Liu, J., Wen, S., Wei, Q., Yan, C., Shi, Y. (2016). Crystal orientation, crystallographic texture and phase evolution in the Ti–45Al–2Cr–5Nb alloy processed by selective laser melting. *Materials Characterization*, 113, 125–133. doi:10.1016/j.matchar.2016.01.012

Liu, Z., Navik, R., Tan, H., Xiang, Q., Wahyudiono, Goto, M., … Zhao, Y. (2022). Graphene-based materials prepared by supercritical fluid technology and its application in energy storage. *The Journal of Supercritical Fluids*, 188, 105672. doi:10.1016/j.supflu.2022.105672

Lu, C., Yang, H., Zhu, C., Chen, X., Chen, G. (2009). A Graphene Platform for Sensing Biomolecules. *Angewandte Chemie*, 121(26), 4879–4881. doi:10.1002/ange.200901479

Lu, S., Wang, S., Wu, P., Wang, D., Yi, J., Li, L., … Pan, H. (2021). A composite prepared from covalent organic framework and gold nanoparticles for the electrochemical determination of enrofloxacin. *Advanced Powder Technology*, 32(6), 2106–2115. doi:10.1016/j.apt.2021.04.025

Luo, Y., Wang, Q. (2014). Zein-based micro- and nano-particles for drug and nutrient delivery: A review. *Journal of Applied Polymer Science*, 131(16). doi:10.1002/app.40696

Mirkin, M. V., Sun, T., Yu, Y., Zhou, M. (2016). Electrochemistry at One Nanoparticle. *Accounts of Chemical Research*, 49(10), 2328–2335. doi:10.1021/acs.accounts.6b00294

Papaderakis, A., Pliatsikas, N., Prochaska, C., Papazisi, K. M., Balomenou, S. P., Tsiplakides, D., … Sotiropoulos, S. (2014). Ternary Pt-Ru-Ni catalytic layers for methanol electrooxidation prepared by electrodeposition and galvanic replacement. *Frontiers in Chemistry*, 2. doi:10.3389/fchem.2014.00029

Phan, T. T. V., Huynh, T.-C., Manivasagan, P., Mondal, S., Oh, J. (2019). An Up-To-Date Review on Biomedical Applications of Palladium Nanoparticles. *Nanomaterials*, 10(1), 66. doi:10.3390/nano10010066

Rümmeli, M. H., Rocha, C. G., Ortmann, F., Ibrahim, I., Sevincli, H., Börrnert, F., … Cuniberti, G. (2011). Graphene: Piecing it Together. *Advanced Materials*, 23(39), 4471–4490. doi:10.1002/adma.201101855

Silva, S. F., Coelho, L., Frazao, O., Santos, J. L., Malcata, F. X. (2012). A Review of Palladium-Based Fiber-Optic Sensors for Molecular Hydrogen Detection. *IEEE Sensors Journal*, 12(1), 93–102. doi:10.1109/JSEN.2011.2138130

Smith, A. T., LaChance, A. M., Zeng, S., Liu, B., Sun, L. (2019). Synthesis, properties, and applications of graphene oxide/reduced graphene oxide and their nanocomposites. *Nano Materials Science*, 1(1), 31–47. doi:10.1016/j.nanoms.2019.02.004

Song, Y., Xu, M., Liu, X., Li, Z., Wang, C., Jia, Q., … Du, M. (2021). A label-free enrofloxacin electrochemical aptasensor constructed by a semiconducting CoNi-based metal–organic framework (MOF). *Electrochimica Acta*, 368, 137609. doi:10.1016/j.electacta.2020.137609

Suzuki, M., Oda, Y., Noyori, R. (1979). Palladium(0) catalyzed reaction of 1,3-diene epoxides. A useful method for the site-specific oxygenation of 1,3-dienes. *Journal of the American Chemical Society*, 101(6), 1623–1625. doi:10.1021/ja00500a058

Wang, H., Yang, Y., Liang, Y., Robinson, J. T., Li, Y., Jackson, A., … Dai, H. (2011). Graphene-Wrapped Sulfur Particles as a Rechargeable Lithium–Sulfur Battery Cathode Material with High Capacity and Cycling Stability. *Nano Letters*, 11(7), 2644–2647. doi:10.1021/nl200658a

Wei, P., Wang, S., Wang, W., Niu, Z., Rodas-Gonzalez, A., Li, K., … Yang, Q. (2022). CoNi bimetallic metal–organic framework and gold nanoparticles-based aptamer electrochemical sensor for enrofloxacin detection. *Applied Surface Science*, 604, 154369. doi:10.1016/j.apsusc.2022.154369

Wu, S., Mao, J., Zhang, Y., Wang, S., Huo, M., Guo, H. (2023). Sensitive electrochemical detection of enrofloxacin in eggs based on carboxylated multi-walled carbon nanotubes-reduced graphene oxide nanocomposites: Molecularly imprinted recognition versus direct electrocatalytic oxidation. *Food Chemistry*, 413, 135579. doi:10.1016/j.foodchem.2023.135579

Yan, C., Zhang, R., Chen, Y., Wang, G. (2017). Electrochemical determination of enrofloxacin based on molecularly imprinted polymer via one-step electro-copolymerization of pyrrole and o -phenylenediamine. *Journal of Electroanalytical Chemistry*, 806, 130–135. doi:10.1016/j.jelechem.2017.10.047

Yang, S., Dong, J., Yao, Z., Shen, C., Shi, X., Tian, Y., … Zhang, X. (2014). One-Pot Synthesis of Graphene-Supported Monodisperse Pd Nanoparticles as Catalyst for Formic Acid Electro-oxidation. *Scientific Reports*, 4(1), 4501. doi:10.1038/srep04501

Yu, Q., Yang, H., Yang, Y. (2024). Fabrication of an electrochemical sensor for the rapid and sensitive detection of enrofloxacin in meat samples. *Journal of Food*

Measurement and Characterization, 18(1), 87–94. doi:10.1007/s11694-023-02149-3

Zadora, G., Brożek-Mucha, Z. (2003). SEM–EDX—a useful tool for forensic examinations. *Materials Chemistry and Physics*, 81(2–3), 345–348. doi:10.1016/S0254-0584(03)00018-X

Zahra, Z., Habib, Z., Chung, S., Badshah, M. A. (2020). Exposure Route of TiO2 NPs from Industrial Applications to Wastewater Treatment and Their Impacts on the Agro-Environment. *Nanomaterials*, 10(8), 1469. doi:10.3390/nano10081469

Zaman, S., Asif, M. H., Zainelabdin, A., Amin, G., Nur, O., Willander, M. (2011). CuO nanoflowers as an electrochemical pH sensor and the effect of pH on the growth. *Journal of Electroanalytical Chemistry*, 662(2), 421–425. doi:10.1016/j.jelechem.2011.09.015

Zereini, F., Alt, F. (Ed.). (2006). *Palladium Emissions in the Environment*. Springer Berlin Heidelberg: Berlin, Heidelberg. doi:10.1007/3-540-29220-9

Zhang, J., Hao, J., Ma, Q., Li, C., Liu, Y., Li, B., Liu, Z. (2017). Polyvinylpyrrolidone stabilized-Ru nanoclusters loaded onto reduced graphene oxide as high active catalyst for hydrogen evolution. *Journal of Nanoparticle Research*, 19(6), 227. doi:10.1007/s11051-017-3924-5

Zhao, H., Li, F., Liu, X., Xiong, W., Chen, B., Shao, H., … Wu, Y. (2015). A simple, low-cost and eco-friendly approach to synthesize single-crystalline LiMn2O4 nanorods with high electrochemical performance for lithium-ion batteries. *Electrochimica Acta*, 166, 124–133. doi:10.1016/j.electacta.2015.03.040

EXTENDED TURKISH SUMMARY
(GENİŞLETİLMİŞ TÜRKÇE ÖZET)

ENROFLOKSASİNİN ELEKTROKİMYASAL ALGILANMASI İÇİN İNDİRGENMİŞ GRAFEN OKSİT KOMPOZİTİNİ DEKOR EDEN PdRu NANOPARTİKÜLLERİNİN YAPISI

IBRAHIM, Aram Hamza
Yüksek Lisans Tezi, Kimya Anabilim Dalı
Danışman: Doç. Dr. Adem ZENGİN
Kasım 2024, 71 sayfa

Bu çalışmada, antibakteriyel olan ve hayvan ile insan sağlığı açısından büyük öneme sahip olan enrofloksasini tespit etmek için sentezlenen pd@Ru/rGO camsı karbon elektrot, paladyum (Pd) ve rutenyum nanopartikülleri (Ru) yüzeye indirgenmiş grafen oksit ile kaplanmış ve Pd@Ru/rGO hazırlandıktan sonra elektron mikroskobu (SEM) ile taranarak incelenmiştir; sonuç olarak, rGO yüzeylerindeki her bir Pd ve Ru nanopartikülünün düzgün, kompakt bir morfolojiye sahip olduğu ve her bir nanopartikülün rGO yüzeyinde homojen olarak dağıldığı, farklı büyütme oranları ve farklı çalışma alanları nedeniyle elde edilmiştir (Şekil 4.1). Pd@Ru/rGO'nun SEM analizi, Pd ve Ru nanopartiküllerinin düşük büyütmelerden yüksek büyütmelere kadar indirgenmiş grafen oksit yüzeylerde homojenlik ve dağılım gösterdiğini göstermiştir. Büyütme; 20.00 KX, 100.00 KX, 200.00 KX'ten başlar ve farklı nanometre dizileri 1 mikron, 200 nm, 100 nm'dir. SEM ve EDX cihazları morfoloji ve yüzey analizi ile ilgilenir (Zadora vd., 2003). Daha sonra EDX cihazları, rGO yüzeyinde paladyum ve rutenyumun düzenli dağılımını tespit etti ve bu dağılım homojen görünüyordu (Şekil 4.2).

Başka bir yüzey analizi olan XRD, kristalin malzemeleri karakterize etmek için etkili bir tahribatsız teknikti. XRD, yapılar, fazlar ve tercih edilen kristal yönelimleri hakkında bilgi elde eder. XRD yöntemi bilim, mühendislik ve teknolojide kritik öneme sahiptir (El Bourakadi vd., 2021a) rGO kaplanmış yüzeydeki her bir nanopartikül elementini tespit etmek ve numunelerin kristalliğini ve saflığını belirlemek için bir XRD cihazı kullanıldı (El Bourakadi vd., 2021b). Bu çalışmada, literatür taramasıyla da benzerlik gösteren bir şekilde, paladyum Pd pikinin $2\theta = 40°$'da, rutenyum Ru pikinin ise $2\theta = 43°$'da ortaya çıktığını gözlemledik (Şekil 4.3) (Zhang vd., 2017; Boukhoubza vd., 2019). Bazı tepeler, kristalin yönelimleri nedeniyle diğerlerinden daha yoğundu; (Şekil 4.3)'te rGO örüntüsünü ve Pd@Ru/rGO'yu incelediğimizde, her bir elementin, Pd ve

Ru'nun, rGO yüzeyinde sabitlendiğini ve Pd@Ru/rGO ürettiğini biliyoruz (W. Li vd., 2016; Q. He vd., 2020).

Bu çalışmada XPS cihazı, XPS ile karakterize edilen Pd@Ru/rGO yüzey analizinin elementel bileşimini belirlemek ve ayrıca her bir nanopartikülün oksidasyon durumunu tespit etmek ve belirlemek için kullanılmıştır. Paladyum ve rutenyum nanopartiküller olarak kullanılmış ve enerji seviyesi ile bombardıman edildiğinde uyarılmış bir duruma dönüşen zemin durumu arasında oksidasyon durumu (0 ila +2) vardır. Ayrıca, her biri tespit edilmiş ve (Şekil4.4) araştırma analizinde ortaya çıkmıştır. Her bir nanopartikülün farklı bir bağlanma enerjisi vardı ve +2 oksidasyon durumunda benzerdi. Paladyumun XPS spektrumu, sırasıyla Pd 3d5/2 ve Pd 3d3/2'ye karşılık gelen 335,1 ev, ve 340,4 ev'de iki tepe göstermektedir (Yang vd., 2014). Bu, Pd'nin, bu çalışmaya benzer şekilde farklı bağlanma enerjilerine sahip olan rGO yüzeyinde kaplandığı anlamına gelir (Şekil 4.4). 285.4 ev, 286. 9 ev , and 289. 4 ev'deki üç tepe, sp3 toplu bağlı karbon C-C, C-O kimyasal bağlarına atfedilir ve C=O bağları, rGO'nun yapısına göre (Şekil 4.4) sp3'te toplu bağlı C1'ler olarak ortaya çıkar (Dolgov vd., 2015) . Şekil 4.3'teki XPS görüntüsünde Ru3d = 284 ev bağlanma enerjisinin analizi, benzer oranda Ru3d = 284 ev bağlanma enerjisi olduğunu da göstermektedir (Papaderakis vd., 2014).

Genel olarak, SEM ve EDX'e göre, XRD ve XPS, Pd@Ru/rGO'nun karakterizasyonunu yüzeysel olarak analiz etmek için kullanıldı. Başarılı bir şekilde sentezlenenin, enrofloksasini tespit etmek için bir elektrokimyasal sensör hazırlamaya hazır olduğunu biliyoruz.

Tablo 5.1, çeşitli modifiye elektrotlar kullanılarak ENR için elde edilen sonuçları sunmaktadır. Daha önce bildirilen çalışmalarla karşılaştırıldığında, üretilen Ru/Pd/rGO/GCE sensörü, düşük bir tespit sınırıyla geniş bir doğrusal belirleme aralığı ve yüksek hassasiyet sergileyerek, indirgenmiş grafen oksit, paladyum ve rutenyum nanopartikülleri arasındaki önemli sinerjik etkiyi vurgulamıştır, bu nedenle bu çalışmada MIP elektrokimyasal elektrotlarla karşılaştırıldığında, bazı MIP elektrotlarından daha iyi enrofloksasin tespiti için elektrotlar (Tablo 5.1) referanslar tarafından onaylanmıştır, ancak yeni elektrokimyasal sensörlerle karşılaştırıldığında, bazı elektrokimyasal sensörler yüksek tekrarlanabilirlik, yüksek yeniden üretilebilirlik, yüksek kararlılık ve hassasiyete göre enrofloksasini tespit etmek için gözlenen elektrokimyasal sensörden daha iyidir, gözlenen elektrot referanslar tarafından onaylanan tabloda yer alan diğer

elektrotlardan daha iyidir, bu nedenle, bu elektrodun Pd@Ru/rGO/GCE'nin enrofloksasin tespiti için başarılı bir şekilde sentezlendiğini önerebiliriz.

Sonuç olarak, bu çalışmada üretilen Ru/Pd/rGO/GCE sensörü kullanılarak ENR belirlendi. Sensör 0.6 ila 116 μM arasında tatmin edici bir doğrusal algılama aralığı gösterdi. LOD değeri $S / N = 3$ baz alınarak 0.2 μM olarak belirlendi. Ayrıca, elektrodun duyarlılığı 0.0291 μA μM'dir. Sensör kullanılan elektroaktif bileşiklere karşı mükemmel seçicilik gösterdi. Elde edilen standart sapmaya, bağıl standart sapmaya ve geri kazanımlara göre mükemmel tekrarlanabilirlik ve yeniden üretilebilirlik gösterdi. Bu sonuçlar göz önüne alındığında, hazırlanan Ru/Pd/rGO malzemesi tatmin edici sonuçlar sergiledi.

Yeni bir özgün elektrokimyasal sensör Pd@Ru/rGO'nun üretilmesi nedeniyle. Üretim elektrot sensörünün durumu ve elektrokimyasal sensöre tepkisi nedeniyle, tablet veya serumdaki diğer antibiyotikleri tespit etmek için paladyum ve rutenyum yerine başka bir platin grubu veya geçiş metali nanopartikülleri kullanmak mümkündür. En önemlisi, yeni elektrotların üretilmesinin bir hata olabilmesidir. Ancak, bu makalede kullanılan her parametrenin durumundaki değişiklikler nedeniyle elektrotların yeteneğini artırabilir.

.

CURRICULUM VITAE

Personal Information

Name Surname : ARAM HAMZA IBRAHIM
E-mail : aramhamza1991@gmail.com

Education Information

Undergraduate
University : Koya University
Faculty : Science and Health
Department : Chemistry
Graduation Year : 2015

VAN YÜZÜNCÜ YIL UNIVERSITY
THE INSTITUTE OF NATURAL AND APPLIED SCIENCES
THESIS ORIGINALITY REPORT

Date 10/12/2024

Thesis Title: CONSTRUCTION OF PdRu NANOPARTICLES DECORATED REDUCED GRAPHENE OXIDE COMPOSITE FOR ELECTROCHEMICAL SENSING OF ENROFLOXACIN

The title of the mentioned my thesis, above having total 71 (Seventy one) pages with cover page, introduction, main parts and conclusion, has been checked by me/my supervisor for originality by Turnitin computer program on the date of 28/11/2024 and its detected similary rate was 20% (Twenty percent) according to the following specified filtering.

The applied filters are given below:

- Excluding the acceptance and approval page,
- Excluding Acknowledgments,
- Excluding table of contents,
- Excluding symbols and abbreviations,
- Excluding materials and methods,
- Excluding references,
- Excluding quotations,
- Excluding publications derived from the thesis
- Excluding the text parts less than 7 words (Limit match size to 7 words)

I read the Thesis Originality Report instruction of Van Yuzuncu Yil University for Obtaining and Using Similarity Rate for the thesis and I declare my thesis does not contain any plagiarism according to the maximum similarity rates specified in this directive; otherwise, I accept all kinds of legal responsibility for any dispute arising in situations which are likely to be detected and I declare that the information I have given above is correct.

I submit it to your information.

Date and Signature
Name and Surname: ARAM HAMZA IBRAHIM 10-12-2024
Student ID: 22910001170
Department: Chemistry
Program: Analytical chemistry
Status: (X) M.Sc. ( ) Ph.D.

SUPERVISOR
SUITABLE

APPROVAL OF THE INSTITUTE
SUITABLE